SOLAR HEATING & COOLING PROGRAMME
INTERNATIONAL ENERGY AGENCY

Catalogue on optimized Solar Energy Buildings

IEA SHC TASK 66 | SOLAR ENERGY BUILDINGS

Technology Collaboration Programme
by iea

SOLAR HEATING & COOLING PROGRAMME
INTERNATIONAL ENERGY AGENCY

Catalogue on optimized Solar Energy Buildings

This is a report from SHC Task 66: Solar Energy Buildings and work performed in Subtask BC: Catalogue on optimized Solar Energy Buildings

Author/Editor
Elsabet Nielsen, DTU – Technical University of Denmark
Simon Furbo, DTU – Technical University of Denmark

September 2024
Report number D.BC3

Cover photo credit Jenni Energietechnik AG, 100% solar-heated multi-family building in Oberburg, Switzerland

Autor/Editor
Elsabet Nielsen and Simon Furbo
Technical University of Denmark (DTU)
Denmark

Contributors

Elsabet Nielsen, Simon Furbo
Technical University of Denmark (DTU)
Denmark

Fabian Ochs, Elisa Venturi
University of Innsbruck
Austria

Stafanie Lott, Harald Drück, Peer Huber
IGTE University of Stuttgart
Germany

Michael Gumhalter, Thomas Ramschak
AEE - Institute for Sustainable Technologies
Austria

Rebecca Yang, Chengyang Liu
Solar Energy Application Lab, School of PCPM, RMIT University
Australia

Xinyu Zhang, Wenbo Cai
China Academy of Building Research (CABR)
China

Franziska Bockelmann, Markus Peter
siz energieplus / dp-quadrat
Germany

Gerhard Mengedoht
Technische Hochschule Ulm (THU)
Germany

Lukas Oppelt
TU Bergakademie Freiberg
Germany

Solar Heating & Cooling Technology Collaboration Programme (IEA SHC)

The Solar Heating and Cooling Technology Collaboration Programme was founded in 1977 as one of the first multilateral technology initiatives ("Implementing Agreements") of the International Energy Agency.

Our mission is: *"Through multi-disciplinary international collaborative research and knowledge exchange, as well as market and policy recommendations, the IEA SHC will work to increase the deployment rate of solar heating and cooling systems by breaking down the technical and non-technical barriers."*

IEA SHC members carry out cooperative research, development, demonstrations, and exchanges of information through Tasks (projects) on solar heating and cooling components and systems and their application to advance the deployment and research and development activities in the field of solar heating and cooling.

Our focus areas, with the associated Tasks in parenthesis, include:

- Solar Space Heating and Water Heating (Tasks 14, 19, 26, 44, 54, 69)
- Solar Cooling (Tasks 25, 38, 48, 53, 65)
- Solar Heat for Industrial and Agricultural Processes (Tasks 29, 33, 49, 62, 64)
- Solar District Heating (Tasks 7, 45, 55, 68)
- Solar Buildings/Architecture/Urban Planning (Tasks 8, 11, 12, 13, 20, 22, 23, 28, 37, 40, 41, 47, 51, 52, 56, 59, 63, 66)
- Solar Thermal & PV (Tasks 16, 35, 60)
- Daylighting/Lighting (Tasks 21, 31, 50, 61)
- Materials/Components for Solar Heating and Cooling (Tasks 2, 3, 6, 10, 18, 27, 39)
- Standards, Certification, and Test Methods (Tasks 14, 24, 34, 43, 57)
- Resource Assessment (Tasks 1, 4, 5, 9, 17, 36, 46)
- Storage of Solar Heat (Tasks 7, 32, 42, 58, 67)

In addition to our Task work, other activities of the IEA SHC include our:

- SHC Solar Academy
- *Solar Heat Worldwide*, annual statistics report
- SHC International Conference

Our members

Australia	European Copper Institute	SICREEE
Austria	France	Slovakia
Belgium	Germany	South Africa
Canada	International Solar Energy Society	Spain
CCREEE	Italy	Sweden
China	Netherlands	Switzerland
Denmark	Norway	Turkey
EACREEE	Portugal	United Kingdom
ECREEE	RCREEE	
European Commission	SACREEE	

For more information on the IEA SHC work, including many free publications, please visit www.iea-shc.org.

Contents

1 Executive Summary

Seven different solutions of Solar Energy Building communities have been investigated by means of calculations with different detailed simulation models. For each solution, parameter variations were carried out to determine optimized solutions.

The calculations included systems in different climates and locations, such as European, Asian and Australian locations.

The solutions can be of inspiration for planners, architects and consultants in connection with planning and designing of future Solar Energy Buildings and communities as well as in connection with renovation of existing buildings and communities.

2 Introduction

This catalogue describes calculations on optimized Solar Energy Building solutions with different simulation programs. The following solutions are included:

- Block of multi-family houses, continental climate (Germany)
- Multi-family solar houses with flat-rate rental model, continental climate (Germany)
- District with multi-family houses, cold district heating network, ice store and solar thermal air-brine collectors, continental climate (Germany)
- Two multi-family houses, moderate climate (Austria)
- Single-family houses, temperate climate (Denmark)
- Office building in Beijing, cold and temperate climate (China)
- Residential/Single dwelling (Josh's House), Warm temperate climate (Australia)

3 Key Performance Indicators

Basis for the definition of the Key Performance Factors (KPIs) is the Energy Flow Diagram (EFD) given in *Figure 1*. The diagram shows all relevant energy flows from primary to useful energy in buildings, blocks and communities. The explanation of the energy flows can be found in the nomenclature list. Generally, "E" stands for electric energy and "Q" for thermal energy. The energy flows, which might be results of simulations, are major inputs to calculate different KPIs. The time intervals for which the KPIs should be calculated are the calendar month and one entire year. However, in addition arbitrary intervals are possible.

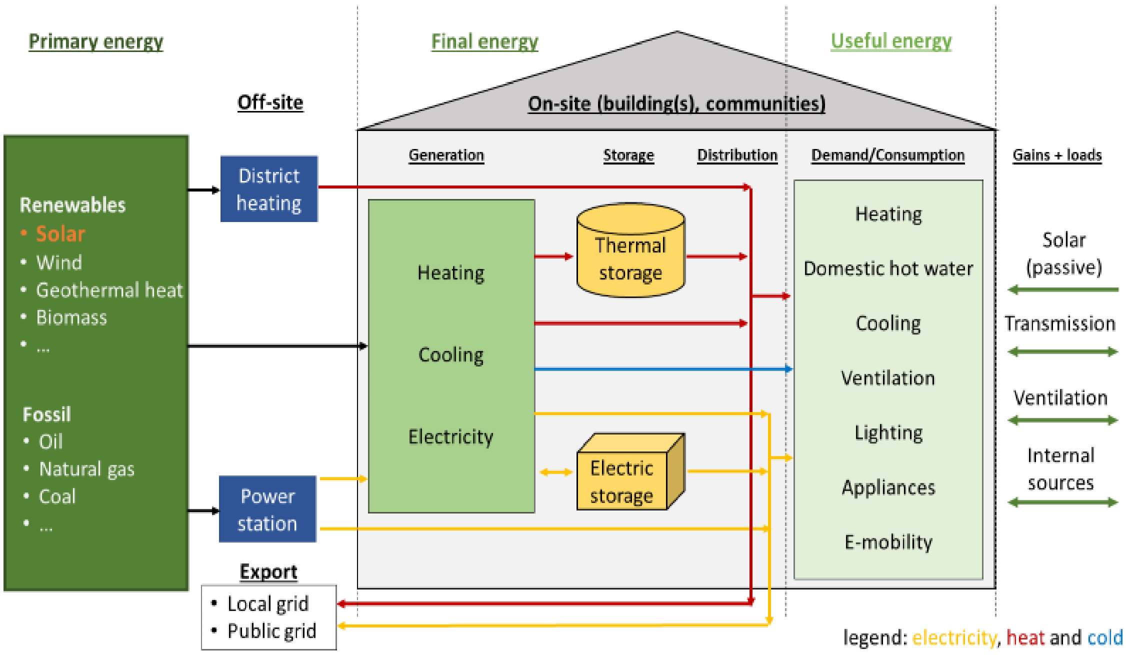

Figure 1: Energy Flow Diagram (EFD) for definition of the Key Performance Factors (KPIs)

All data included in one KPI must refer to the same time interval. In the context of the list on hand, the basis of all KPIs are simulation results. If applicable the KPIs should also be used in case of cooling. In this context ""KPI thermal"" means the definition of KPIs for heating and cooling."

The fields of observation and boundaries of the different KPIs correspond to the focus Task 66 is aiming at. Thus KPIs for buildings, blocks and communities that are investigated by different Task participants, should be an outcome.

Participants may feel free to add intermediate steps and/or individual areas within their systems and calculate belonging, more specific KPIs, e. g. renewable, electrical, thermal etc."

When calculating KPIs the documentation of relevant boundary conditions as well as specifics of the simulation (e. g. simulation program, time step of simulation and the location of building site) is mandatory.

To contrast values of different projects and/or between Task 66 participants both monthly and yearly values of the listed KPIs are desirable. Beside the given KPIs other data, e.g. on weekly or monthly basis, might be advantageous to show and explain particular findings around a particular concept."

Ecologic KPIs:

These KPIs might even be more strongly connected to the country or region in which the system under investigation is located. Due to this in particular documentation of all relevant boundary conditions but also of specifics of the simulation is important. For further information refer to the report of Subtask A: Boundary conditions, KPIs, definitions and dissemination,

Filename: Task66_D.A2_Final list of KPIs_1.3; Report number D.A2, DOI; Date 13/12/2022"

When calculating economic and ecologic KPIs it is advantageous to refer to the same boundary conditions and assumptions, e. g. lifespan of products and time frame of investigation.

To allow for best possible comparison to other cases, like single buildings or building blocks, KPIs should refer to specific values, e. g. (tons for CO2equivalent)/(m^2 a). Reference values, such as areas, have to be defined precisely, e. g. net floor area, gross floor area, etc.

Preferably the evaluation of simulation results and calculation of KPIs shall be based and referred to square meter gross floor area (m^2GFA).

For calculation of the gross floor area, external measurements of the building structure shall be used.

Table 1: KPIs for simulations

KPI No.	Name	Definition	Remarks
1	Useful energy Q_{cons} and E_{cons} [kWh]	Q_cons=Q_(SH/SC)+ Q_DHW E_cons= E_HH+E_HE+E_HP+E_mobil+E_light+E_aux Useful energy demand/consumption of a building including all thermal energy (like domestic hot water, space heating) and all electrical energy, for example household, mobility and auxiliary*) energy as well as heat pump or heating element. *) refer to abbreviations	
2	Final energy Q_f [kWh]	Q_f=Q_del+ E_grid+Q_ST-Q_(ST,grid)+E_(PV,tot)-E_(PV,grid) Final energy demand/consumption of a building, including all electrical and thermal energy as well as other energy for producing heat, cold and electricity. If necessary, the renewable share of the supplied energy can be specified further.	
3	Grid feed-in E_{grid} and / or Q_{grid} [kWh]	E_(PV,grid) ; E_(CHCP,grid) Q_(ST,grid) ; Q_(CHCP,grid) Solar or electrical energy production on side, which is feed into the local grid.	Probably ST will be feed into a grid only to a limited extent. If applicable, include it.
4	Passive solar gains QSP,gain [kWh_{th}]	Passive solar gains might be determined by simulation.	In principle, this can be done by simulating the building including all technical facilities and boundary conditions twice, with and without exposed to solar (radiation). The difference between the results are passive solar gains.
5	Total solar fraction = LCF – Solar Load Cover Factor [%]	*f_sol = (E_(PV,tot)-E_(PV,grid)+Q_(ST,tot)-Q_(ST,grid))/(E_(PV,tot)-E_(PV,grid)+E_grid+Q_(ST,tot)-Q_(ST,grid)+Q_grid+Q_h-Q_(h,el))* Fraction of self-generated and self-used PV electricity and useful heat from solar thermal referred to the total energy used for household and technical purposes.	Important for checking the objectives in Task 66
6	Solar fraction thermal = LCF_{th} – Load Cover Factor [%]	f_(sol,th)=(Q_(ST,tot)-Q_(ST,grid)+ Q_(sol,PVHG))/(Q_(ST,tot)-Q_(ST,grid)+Q_DH+Q_h) Fraction of solar-generated useful heat referred to the total heat consumption. Direct solar thermal applications as well as solar electric heat generators (e. g. heat pump with photovoltaic power) are considered.	Important for checking the objectives in Task 66
7	Solar fraction electrical = LCF_{el} – Load Cover Factor [%]	*f_(sol,el)=(E_(PV,tot)-E_(PV,grid))/(E_(PV,tot)-E_(PV,grid)+E_grid)* Fraction of electricity generated by a photovoltaic system referred to the total electricity consumption.	Important for checking the objectives in Task 66
8	SCF_{ST} – supply cover factor ST [%]	*SCF_ST = Q_(ST,use)/Q_(ST,tot) with Q_(ST,use)= Q_(ST,tot) - Q_(ST,grid)* Supply cover factor for solar thermal use. Only possible to use this KPI, when energy can be fed into the grid.	Probably ST will be feed into a grid only to a limited extent. If applicable, include it.
9	SCF_{PV} – supply cover factor PV [%]	SCF_PV = E_(PV,use)/E_(PV,tot) with E_(PV,use)= E_(PV,tot) - E_(PV,grid) Supply cover factor for solar electrical use.	
10	Non-renewable final energy saved [kWh/a]	difference to the *reference case* or between variants, for system operation only	Difference(s) between the variants on the energy balance (final energy) should be documented (electricity, gas, oil, biomass, heat etc.).
11	Reduced greenhouse gas emissions (GWP100) [t-CO_2-eq/a]	Difference(s) to *reference case(s)* or between variants. For system operation only. Monthly but at least annually values of country-specific and/or commonly used CO_2 equivalents.	Documentation of all used conversion factors (CO_2 emission factors), general and/or local ones (monthly and/or annually conversion factors). It has to be stated, whether the conversion factors are general or local. Example for calculating CO_2 emissions CO_2-emission = Q_f x CO_2-emission factor depend on gas, electricity or …

4 Investigations

The investigations are theoretical and performed on different simulation platforms including TRNSYS, POLYSUN and MATLAB-Simulink.

4.1 Investigated systems

Table 2 lists the investigated cases, the location of the cases and the parameter variations conducted.

Table 2: Investigated cases

System number	System	System diagram	Variations
5.1	Block of multi-family houses, continental climate (Germany).	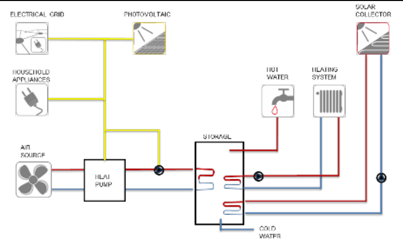	Space heating demand Building orientation Energy storage size Solar energy system area PV/ST area ratio PV/ST orientation PV tilt PV/ST efficiency
5.2	Multi-family solar houses with a flat-rate rental model, continental climate (Germany)	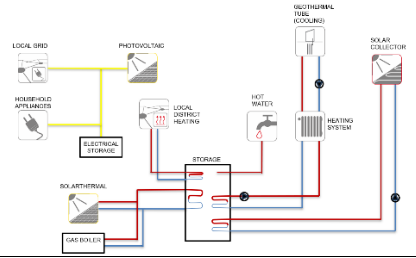	PV power ST area Electrical storage capacity Heat storage volume Building location
5.3	District with multi-family houses, cold district heating network, ice store and solar thermal air-brine collectors, continental climate (Germany)	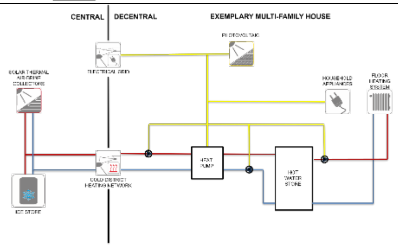	Ratio between heating demand and Ice store's thermal capacity
5.4	Two multi-family houses, moderate climate (Austria)	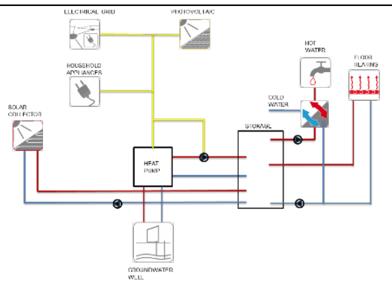	ST replaced by PV Buffer storage operation Appliances included
5.5	Single-family houses, temperate climate (Denmark)	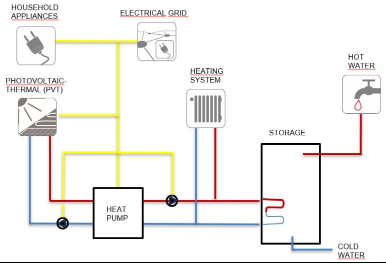	Space heating demand PVT tilt PVT area Electrical storage capacity

5.6	Office building in Beijing, cold and temperate climate (China)	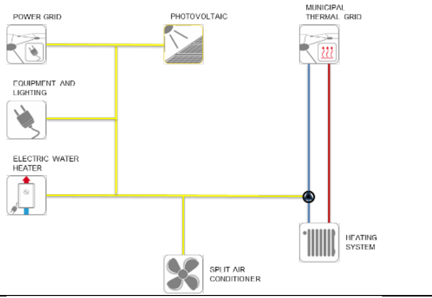	PV shading PV type PV orientation PV tilt
5.7	Residential/Single dwelling (Josh's House), warm temperate climate (Australia)	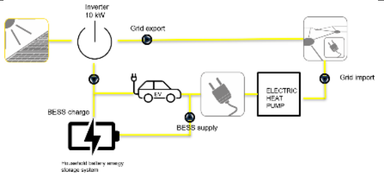	PV tilt PV area

5 Details and results of systems

In the following sections, the different investigated systems are presented in detail.

5.1 Block of multi-family houses, continental climate (Germany)

5.1.1 Building and System

Table 3 shows the building and system data used as the starting point of the simulations and study. In chapter 5.1.3 all variants are listed.

Table 3: Building and system data for Block of multi-family houses

Building Data	
Location	Potsdam (Germany)
Building	Multi-family house
Energy ref. area	1,440 m² (NFA)
Useful energy (Q_{cons} and E_{cons})	
Heating demand	46.3 kWh/(m²a)
Cooling demand	- kWh/(m²a)
DHW demand	12.0 kWh/(m²a)
Household demand	18.1 kWh/(m²a)
E-mobility demand	- kWh/(m²a)
Total heating demand	61.1 kWh/(m²a)
Total electricity demand	35.8 kWh/(m²a)
Final energy (Qf)	35.8 kWh/(m²a)
System Data	
Heating generator	Air-source heat pump
Colling generator	none

PV	Total area Number of modules (placed) System efficiency (including all periphery) Peak power	~ 160 m² 2 x 110 modules on the roof 16.2 % 59,2 kWp
Solar thermal	Total area Total aperture area Thermal capacity Collector type	- m² - m² - W -
Thermal storage	Volume	4 x 1,000 l
Electrical storage	Capacity Storage type	30 kWh Lithium Ionen
Ventilation system	System Air change Heat recovery	Natural ventilation / windows - 1/h - %
Heating system	Floor heating	
DHW preparation	Fresh water station	
Cooling system	none	

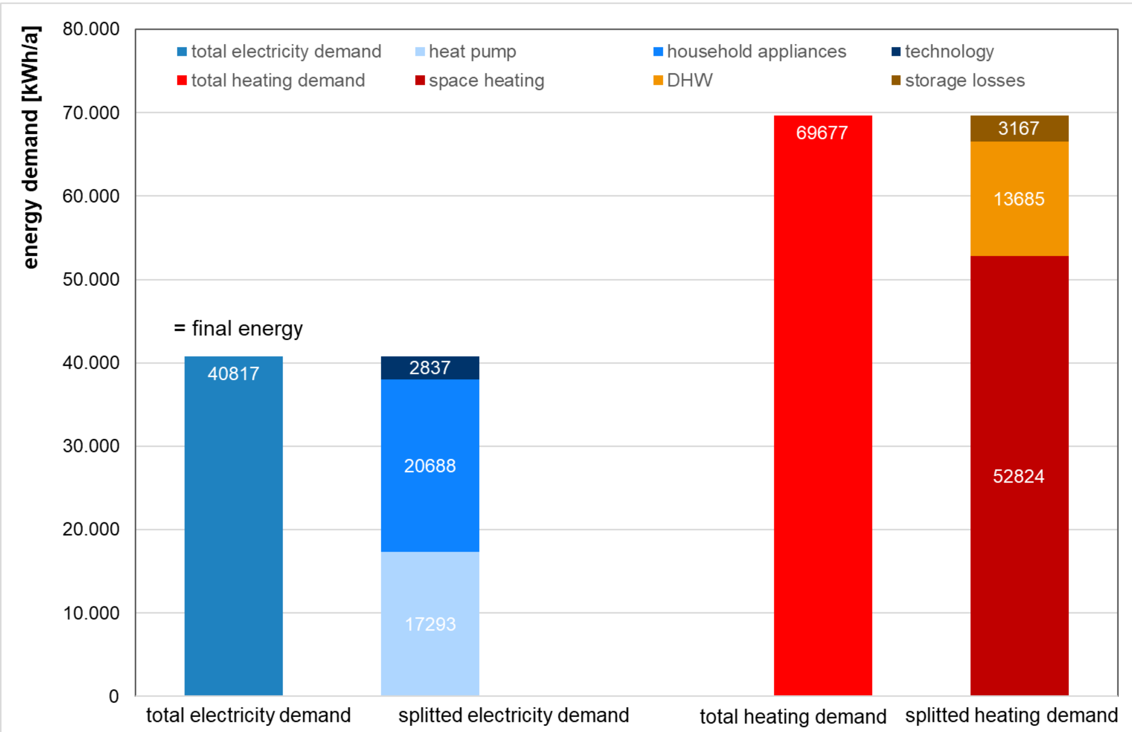

Figure 2: Electricity demand and demand of thermal energy of the building

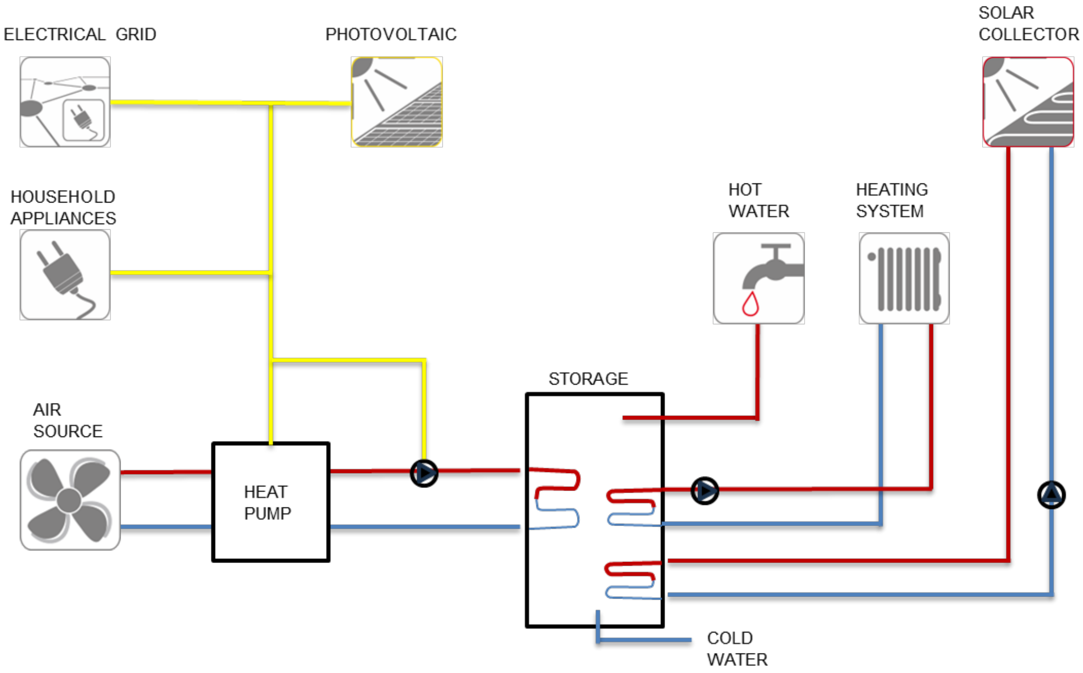

Figure 3: energy concept and systems

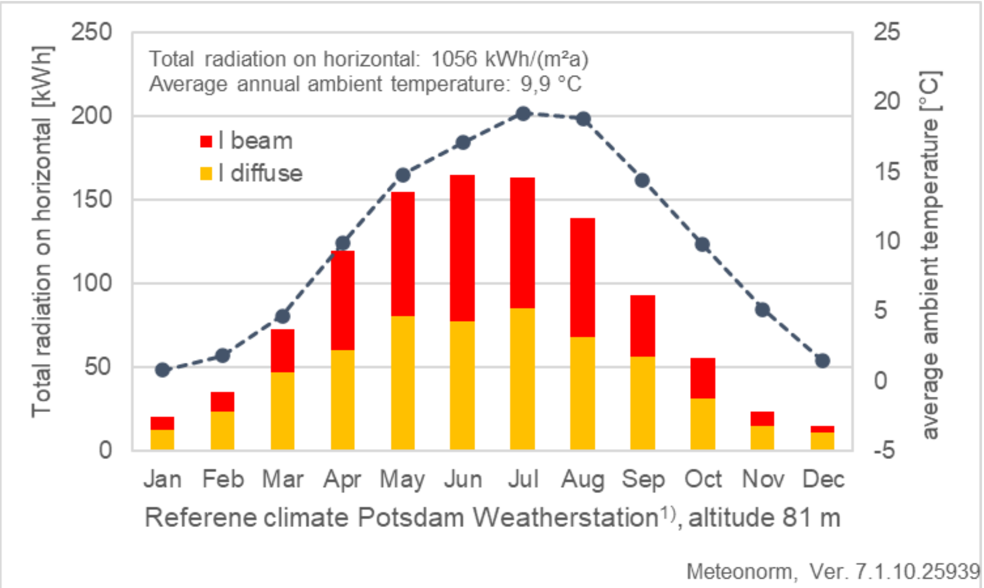

Figure 4: Weather data Potsdam (Germany), average ambient temperature and solar radiation on horizontal

5.1.2 System heat management philosophy/control strategy

The heat supply for both houses is provided by air-to-water heat pumps. The heat pumps operate the heating circuit in the low-temperature range (underfloor heating) and provide domestic hot water for the bathroom and kitchen. A decentralized mechanical exhaust air system increases living comfort. Natural ventilation via the windows is possible at all times. A photovoltaic system and a battery are provided to support the power supply. The remaining electricity required for household and technical purposes is drawn from the public grid.

As soon as the PV system produces electricity, it is allocated as follows / in the following order:

1. household appliances
2. heat pump (compressor)
3. heating element (if available)
4. system technology (e.g. circulation pumps)

5. charging the battery

6. grid feed-in

If possible, demand is always covered by the PV system first. If the PV power is not sufficient, the power from the battery is used first. Only last, if there is further demand, electricity is supplied from the grid.

With regard to solar thermal energy, the simulations proceed as follows: If required, the DHW storage is charged first by the solar system (separate tanks are integrated for DHW and space heating).

The domestic hot water priority circuit also applies to the heat pump.

5.1.3 Simulation variations

With regard to the regenerative cover factor of the entire energy demand (solar thermal and solar electric), the simulation study determines the variant for which, by a complementary distribution of the shares of solar thermal and photovoltaics on the available roof area, the renewable energy used in the building is maximized. In addition to the varying proportions of solar thermal collectors and PV area, the influences of the different ratios combined with unlike thermal and/or electrical storage have been investigated. Since the influence of selected building physics is also to be evaluated, the thermal insulation of the building, in addition to the technical variants, is altered. (see Table 4)

Table 4: Simulation variants

Variation	Starting point	Changes/ adaptions
thermal building standard	as build, no changes apart from insulation and heat recovery of air change for the passive house	“average“– 46.3 kWh/(m²a) = as build (GEG) "good“ – 30 kWh/(m²a) "very good” = passive house – 15 kWh/(m²a)
orientation of the building	orientation of PV and ST similar to building	rotation: 0°, 30°, 60° and 90°
varying storage size	as build	50, 100 and 150 l/m² referred to aperture area of the thermal collector 0, 0.5, 1.0 and 2.0 kWh/kW$_p$ (usable capacity of electrical energy storage)
expansion of the area available / solar active area	initial area 108 m² (as build)	add 50 % (new area 162 m²) correspond to approx. 80 % of the roof area
varying the area shares of PV and ST	PV and ST (assembly on usable roof area)	0 %/100 % to 100 %/0 % (10 % steps) as shown by the first simulations with the system as build, a high total solar fraction is reached in a range between 20/80 and 80/20 -> used for further simulations
orientation of PV and ST	building orientation south PV and ST tilt angle 65°	orientation PV east / west and ST south
varying the tilt angel of PV	building orientation south	ST – unchanged, tilt angle 65°, orientation south PV –tilt angle 30°, orientation south PV – tilt angle 10°, orientation east/west (tilt angle according to pre-study)
varying efficiency (better components)	initial situation (as build) PV - 16,1 % ST – conventional plate collector	PV – 24 % (very good) (source: technology radar Subtask D) ST – high performance CPC-collector

5.1.4 Results

5.1.4.1 Influence of electrical and thermal storage sizes

When considering the capacity of an electrical energy storage, it was found, that the in practice widely used capacity of 0.5 to 1.0 kWh/kW$_p$ has a noticeable influence on the overall system performance and increases the solar-electric fraction. The capacity of 2.0 kWh/kW$_p$ has a significantly higher influence but also the financial outlay increases significantly as well.
As the design value for the simulations on hand a value of 1.0 kWh/kW$_p$ was implemented.
With regard to the specific volume of the hot water store, for the multi-family house under investigation a sensitivity analysis including a flat plate collector results in a reasonable value of 100 l/m², referred to the aperture area of the thermal collector. In that case a specific storage volume of more than 100 l/m² does not lead to a significant increase in the performance of the solar thermal system. On the other hand, a specific volume of 50 l/m² decreases the solar fraction of the system by around 5 percentage points, compared to that with 100 l/m².

5.1.4.2 Influence of thermal insulation and orientation of the building

Of course, the better the thermal building standard, the less energy for space heating and by this less electricity for the heat pump is needed. Furthermore, it is clear that the further the house is turned from south orientation to west (or east), due to decreasing passive solar gains, the more energy for space heating is required. With better thermal insulation of the building (lower energy demand for space heating), the orientation to south results in higher solar fractions. Moreover, the ratio between produced energy and energy demand increases. By enhancing the thermal insulation of the building and turning the building to the south, a total solar fraction of up to 45 % can be achieved (*Figure 5*). In this case the maximum thermal solar fraction amount to 45% (extrapolated) and the electrical solar fraction (PV) to 40 % (extrapolated) (*Figure 6*).

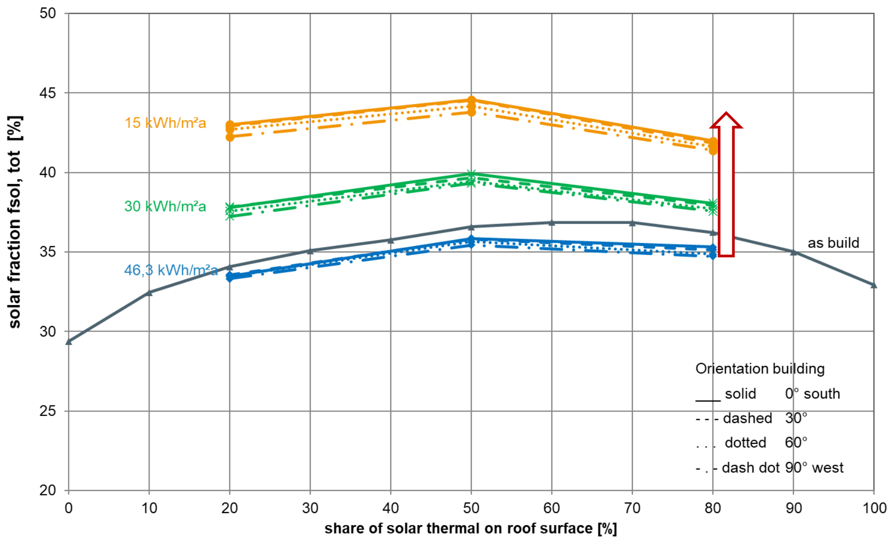

Figure 5: Total solar fraction – thermal insulation and orientation of building

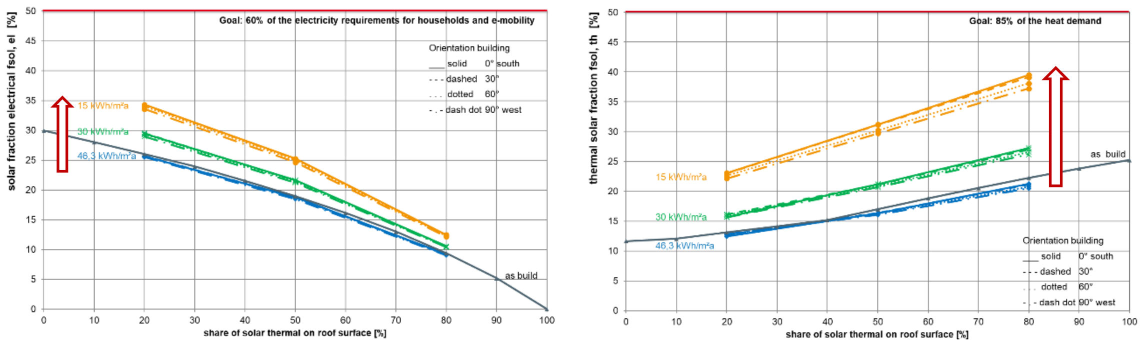

Figure 6: Electrical solar fraction (left) and thermal solar fraction (right) – thermal insulation and orientation of building

5.1.4.3 Influence of orientation und tilt angle on the system performance (PV and ST)

An orientation to south provides the highest solar irradiation and therefore, at first glance, the highest yield. If the tilt angle of a south oriented PV module and a thermal solar collector is adapted to archive the highest yield, of course the highest solar fraction will be reached.

By orienting the systems to south and modify the tilt angle (starting point see Table 1), a total solar fraction of up to 45 % can be achieved (Figure 7). The maximum thermal solar fraction amount to 45 % (extrapolated) and the electrical solar fraction to 42 % (extrapolated) (Figure 8).

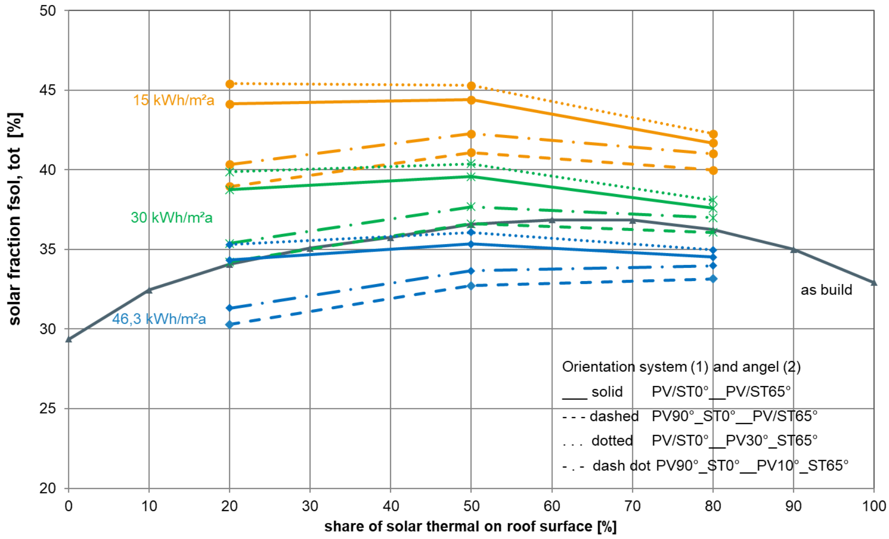

Figure 7: Total solar fraction – orientation and tilt angle of solar appliances

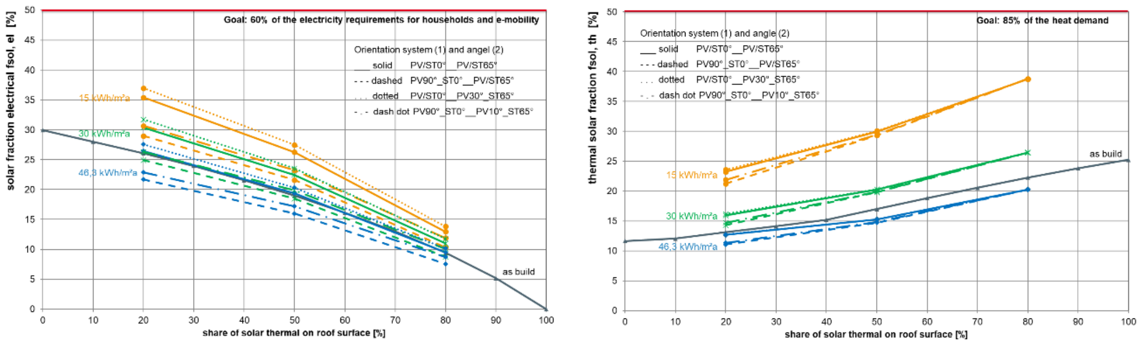

Figure 8: Electrical solar fraction (left) and thermal solar fraction (right)– orientation and tilt angle of solar appliances

5.1.4.4 Influence of efficiency and area of solar applications (PV and ST)

Self-evident the higher the efficiency and the area of solar applications, the more energy can be generated and the higher the solar fraction will be.

By altering the efficiency and the area of solar applications in a range that is feasible for the given building (starting point see Table 4), a total solar fraction of up to 70 % can be achieved (Figure 9). The maximum thermal solar fraction amount to 70 % and the electrical solar fraction to 72 % (Figure 10).

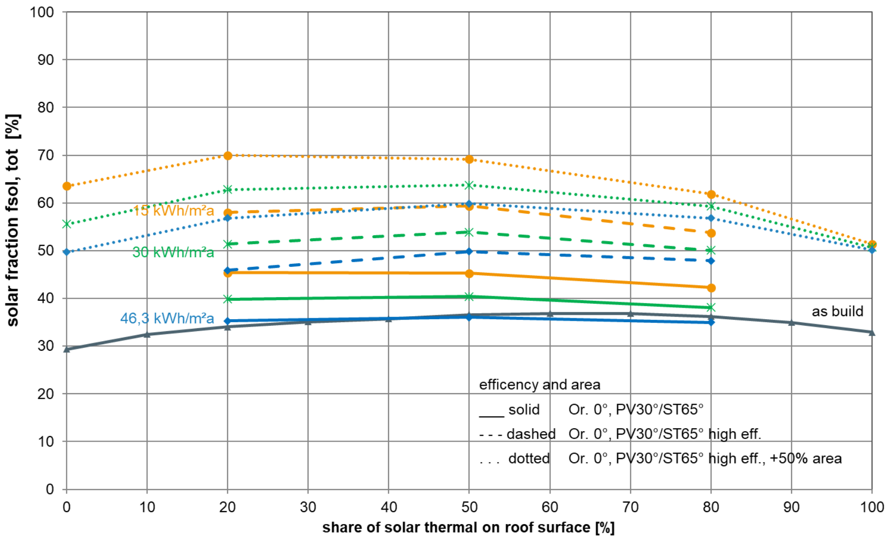

Figure 9: Total solar fraction – efficiency and area of solar appliances

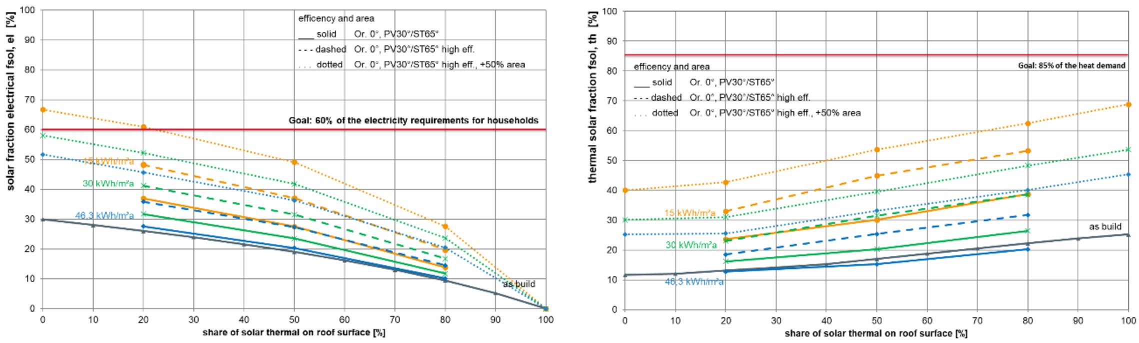

Figure 10: Electrical solar fraction (left) and thermal solar fraction (right) – efficiency and area of solar appliances

5.1.4.5 Supply cover factor – solar thermal and PV

The supply cover factor for solar thermal is 100 % in every variant and every ratio. All the energy produced by the installed solar thermal system is used in the building or temporarily stored in the storage tank.
There is no connection to a heating network.

In contrast, the electricity from the PV system can also be fed into the public grid. Depending on the variant, the supply cover factor for PV is between 44 and 98 %. The larger the PV field or the more PV electricity is produced, the smaller the cover factor becomes. See also in chapter 5.1.4.6 - grid feed-in.

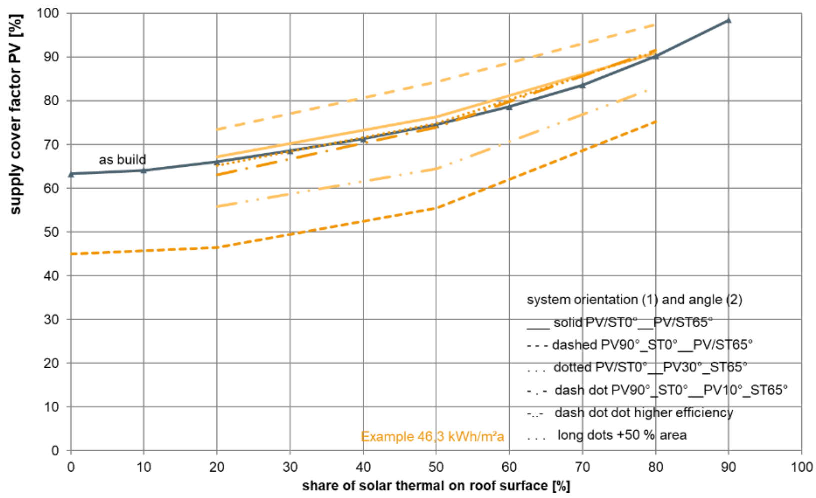

Figure 11: Supply cover factor for PV system

5.1.4.6 Energy production, feed-in and electricity purchase from the local grid

The adaptations of the supply concept and system components mostly result in different energy productions in terms of electricity and heat. By improving the system, the yields generally increase (Figure 12). If the concepts are adapted according to the mentioned outcomes, the electricity production increases by 144 % that of heat by 48 %.

Since the reduction of the use of fossil fuels was a goal underlying the strive to reach high solar fractions, the results show that some adjustments in parallel lead to reduced electricity purchase from the grid. Electricity purchase from grid can be reduced by up to 30 %, depending on the measures implemented. At the same time, the feed-in of surplus electricity into the public grid increases by 267 %. This can support increasing the share of renewable energy in the grid and might in addition have network-friendly effects. (Figure 13)

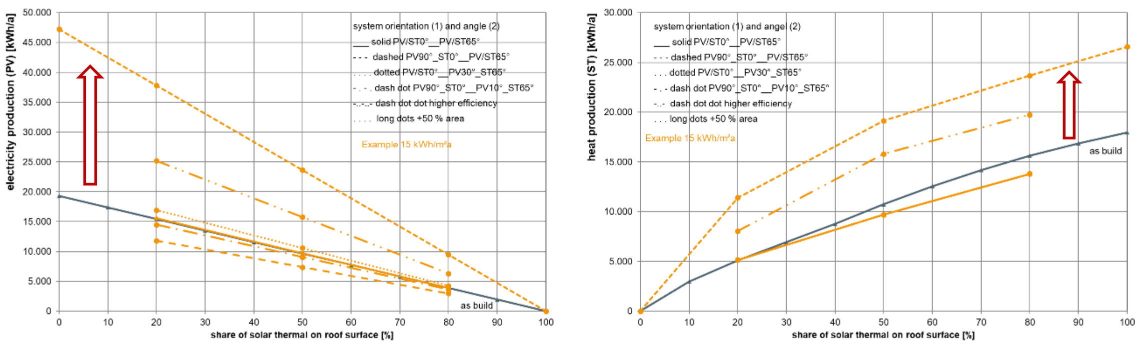

Figure 12: Electricity production (PV) (left) and heat production ST (right)

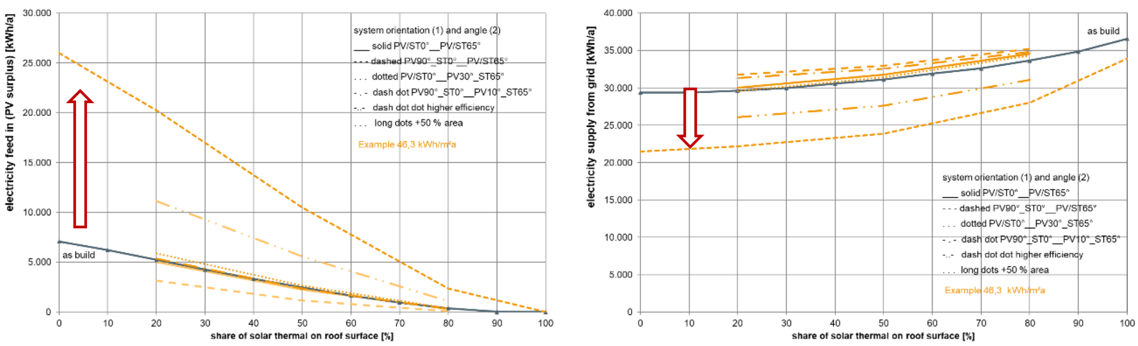

Figure 13: Electricity feed in the grid (left) and grid supply (right)

5.1.4.7 Greenhouse gas emissions (GWP100)

Since reducing the use of fossil fuels is a goal that underlies the drive to reduce CO2 emissions, there are parallels between grid consumption and CO2 reductions. The results for GWP are the same as those for grid procurement. CO2-emission can be reduced by up to 30 %, depending on the measures implemented.

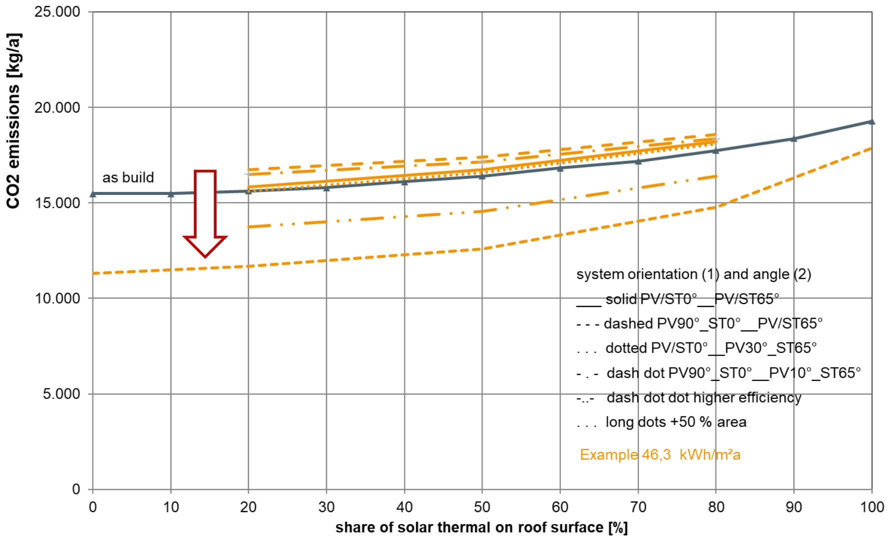

Figure 14: CO2 emissions (without

5.1.5 Conclusion - Outcomes

Outcome of the variants for reaching SEB:

- A thermal store of 100 l/m² aperture area of a thermal collector. With respect to the photovoltaic system an electrical storage with a useful capacity of 1 kWh/kW$_p$ has been implemented.
- A low energy building (15 kWh/m²a) with orientation south is advantageous.
- PV modules and solar thermal collectors should be oriented to south. PV should have a tilt angle of 30°, while the tilt angle of solar thermal collectors should be 65°.
- The efficiency and area of PV and ST should be as high as possible. To approach and reach the goals stated in Task 66 for the given building, the ratio of the net floor area to the area of solar applications (PV and ST) for the 15 kWh/(m²a) building must not be larger than 7. The 30 kWh/(m²a) building is approaching the Task 66 target, while the 46.3 kWh/(m²a) building needs much more solar area.
- The feed-in of surplus PV electricity into the public grid decreases with an increase in the size of the solar thermal system because less PV electricity is produced.
- Enhancing the system might lead to reduced electricity supply from the grid. The electricity supply for the building can be reduced by up to 30 %.
- At the same time, the feed-in of surplus electricity into the public grid increases by more than 250 %. This can support increasing the share of renewable energy in the grid and might in addition have network-friendly effects.

With regard to the solar fractions (with all measures included), the following results can be presented:

Solar fraction	**Concept results** (with all measures included)
total **up to 70 %**	Variants with high total solar fraction range from a ratio between ST and PV of around 20/80 to 50/50. The total solar fraction increases with the size of the solar thermal collector, but to be able to cover household electricity, a minimum proportion of photovoltaics should be available.

thermal **up to 70 %**	It is evident that electricity-oriented heat generation benefits from PV systems. As the PV system becomes smaller, this fact of an electricity-oriented concept is reduced. On the other hand, due to its greater area efficiency, a solar thermal application may overcompensate this effect. Of course, the maximum thermal solar fraction is generated by a ratio of ST to PV of 100/0.
electrical **up to 65 %**	The smaller the PV area, the lower the share of solar electricity coverage. Self-evident, the maximum electrical solar fraction is generated by a ratio of ST to PV of 0/100. To reach the target for the 15 kWh/(m²a) building, the ratio between net floor area and PV area should be around 7. For buildings with higher energy demand, a ratio lower than 7 is mandatory.

5.1.6 References

Bockelmann, F., Peter, M., Oliver, A. Bestenlehner, D., Drück, H., 2019. Final report “Solsys - Analyse und Optimierung solarer Energieversorgungssysteme (Wärme/Strom) für Gebäude“, BMWi Fkz 0325558A/B

Meteonorm® 7, 2018, Global Meteorological Database for Engineers, Planners and Education, Version 7.1.10.25939, Meteotest, Bern (CH)

TRNSYS 17, TRaNsient SYstem Simulationprogramm, Version 17.02.0004, Solar Energy Laboratory, University of Wisconsin-Madison

5.2 Multi-family solar houses with a flat-rate rental model, continental climate (Germany)

Table 5 shows building and system data used as the starting point of the simulations and study. In chapter 5.2.2 all variants are listed.

Table 5: Building and system data for Block of multi-family houses

Building Data		
Location	Cottbus (Germany)	
Building	Multi-family house	
Energy ref. area	854 m² (NFA)	
Useful energy (Q_{cons} and E_{cons})		
Heating demand	60.9 kWh/(m²a)	
Cooling demand	5.7 kWh/(m²a)	
DHW demand	22.3 kWh/(m²a)	
Household demand	19.6 kWh/(m²a)	
E-mobility demand	- kWh/(m²a)	
Total heating demand	85 kWh/(m²a)	
Total electricity demand	23.7 kWh/(m²a)	
Final energy (Qf)	106.6 kWh/(m²a)	
System Data		
Heating generator	Solar thermal and gas boiler	
Colling generator	Geothermal tube	
PV	Total area Number of modules (placed) Peak power	~ 172 m² ~ 111 m² (roof), ~ 61 m² (fassade) 29,6 kWp
Solar thermal	Total area Collector type	100 m² Flat plate collector
Thermal storage	Volume	24,6 m³

Electrical storage	Capacity Storage type	46.8 kWh Lithium Ionen
Ventilation system	System Air change Heat recovery	Ventilation system - 0,5/h - %
Heating system	Floor heating	
DHW preparation	Fresh water station	
Cooling system	Over floor heating system	

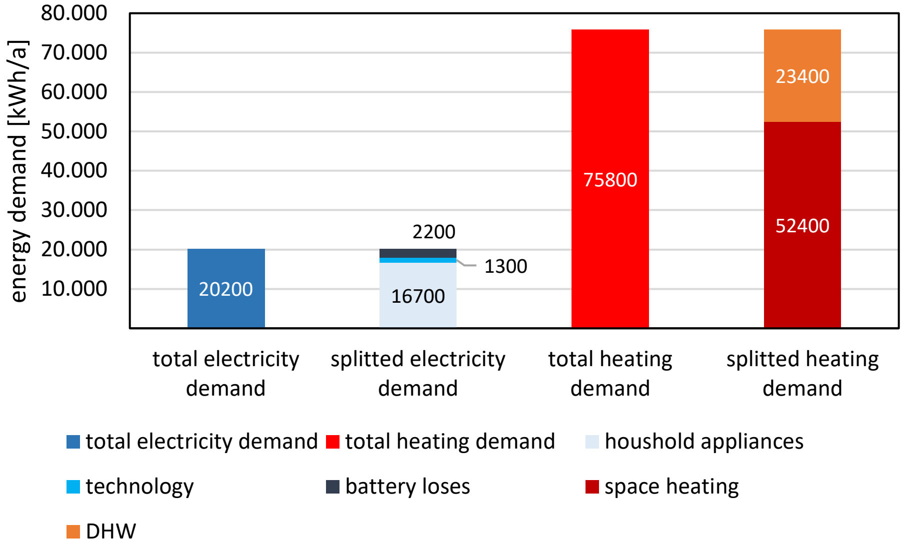

Figure 15: Electricity demand and demand of thermal energy of the building

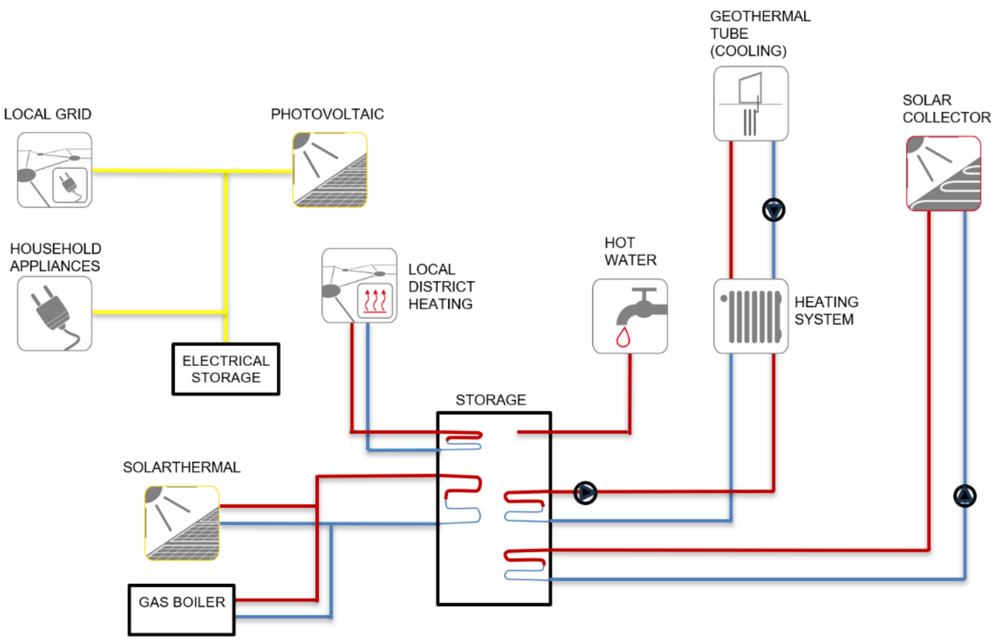

Figure 16: energy concept and systems

5.2.1 System management philosophy/control strategy

A total of two identical multi-family houses of seven units each were built in 2019 in Cottbus (Germany). These are also simulated in this study. The connection in the district with three other apartment buildings (on the heating side) and an office building (on the electricity side) is also partially considered.

Electricity is generated by a PV system and can be temporarily stored in an electricity storage unit. Surpluses are fed into the local grid in the district. If the electricity from the PV system is not sufficient, electricity is supplied from the public grid via the local electricity grid.

On the heating side, heat is provided by a solar thermal system; if this is not sufficient, additional heat is provided by a gas boiler. Solar energy can also be stored in a buffer tank. When this is full, the surplus is transferred to the surrounding area for hot water.

In addition, a geothermal tube can be used for cooling in summer.

5.2.2 Simulation variations

Regarding solar fraction, the first step is to vary the PV power and battery capacity on the power side and the solar thermal area with the thermal storage volume on the thermal side for an individual building. In the second step, the neighbourhood is considered, considering the interconnection of the buildings and the respective solar fractions for the whole district.

In addition, the influence of the location in Germany on the buildings is analysed. For this purpose, the model is simulated for three locations in Germany. The variance of the sizes is listed in Table 6. The simulation was carried out with Matlab Simulink.

Table 6: Simulation variants

Variation	Starting point	Changes/ adaptions
varying the power of PV	as build = 100 %	0 to 3,5 kWp/MWh normalised to total electricity consumption in 20% increments between 0 and 200 % of the installed power
varying the area of ST	as build = 100 %	0 to 5 m²/MWh normalised to total heating consumption in 20% increments between 0 and 200 % of the installed area
varying the capacity of electrical storage	as build = 100 %	0 to 6 kWh/MWh normalised to total heating consumption in 20% increments between 0 and 200 % of the installed area
varying the capacity of thermal storage	as build = 100 %	0 to 1,2 m³/MWh normalised to total heating consumption in 20% increments between 0 and 200 % of the installed area
Location of the building	Cottbus	Transfer of the building model with built parameters from Cottbus (Central Germany) to the locations Hamburg (Northern Germany, near the sea) and Munich (Southern Germany, Alpine)

5.2.3 Results

5.2.3.1 Influence of collector areas and storage tank sizes

Figure 17 shows the solar fraction for each parameter combination for House 1 (left) and House 2 (right).

To ensure the comparability and transferability of the results, the PV power, and the battery capacity are related to the annual electricity consumption of the building, which is about 16.8 MWh/a in both houses. It is not possible to increase the rooftop PV system without reducing the ST system, while the battery capacity could be easily varied. Alternatively, PV systems could be installed on the other buildings in the quarter.

Figure 5.17 shows that a further increase in battery capacity for the same PV power would result in only a small improvement in the solar fraction of the electricity solar fraction. Reducing the battery capacity by 40% to 31.2 kWh (1.9 kWh/MWh) in House 1 results in only a small reduction in the degree of solar fraction to 77%.

In House 2, the solar fraction is already 77% [Oppelt et al. 2022]. To achieve the same level in House 2, the effects of shading can be offset by installing a 40% higher battery capacity. A further increase of the solar fraction is possible in both houses by increasing the peak PV power, but this is very costly: doubling the peak PV power only increases the solar fraction by about 10 percentage points.

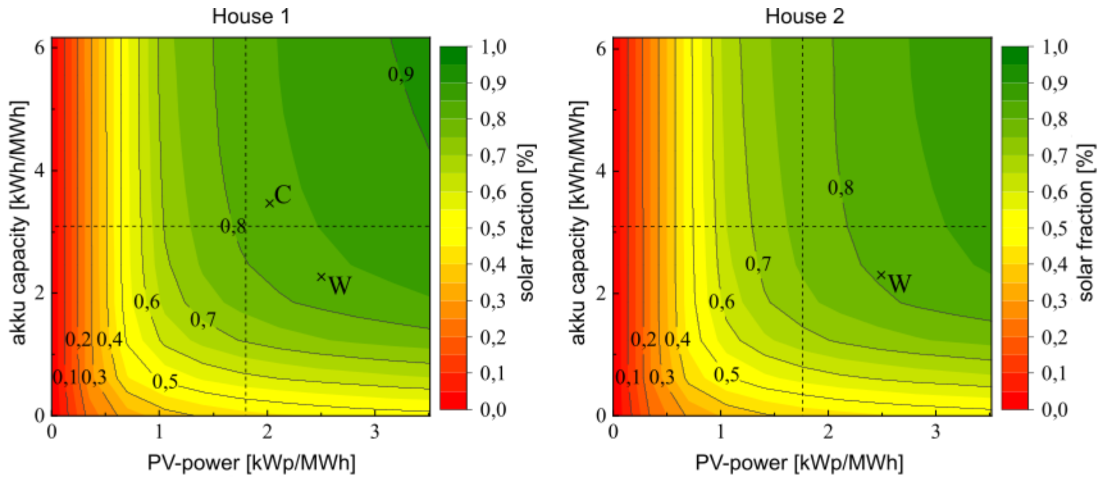

Figure 17 Simulation results of the solar fraction of electricity normalised to annual electricity consumption (approx. 16.8 MWh), dashed line shows initial situation; C : solar fraction resulting from measured consumption in Cottbus (house 1); W : comparative value according to Weniger et. Al 2015

The parameter variation for the heat supply is shown in Figure 18.

Using the actual measured values in House 1 for the annual heat consumption, Figure 18 (left) shows a solar fraction of about 70%, which would result from this consumption in the model.

One reason for the deviation from the measured solar fraction of 60% is the different distribution of heat consumption between heating and hot water in the model and in reality.

Storage volumes greater than 0.33 m³/MWh (15 m³ in the Cottbus house) lead to very small improvements in the solar fraction. Below 1.5 m²/MWh absorber area (60 m²), a storage tank of 5 m³ is sufficient, as a larger tank no longer leads to an improvement in the solar fraction, which even decreases due to increased heat losses through the tank wall (e.g. at isoline 0.3 in Figure 18 (right)). In this case, the ST system can only meet the daily demand.

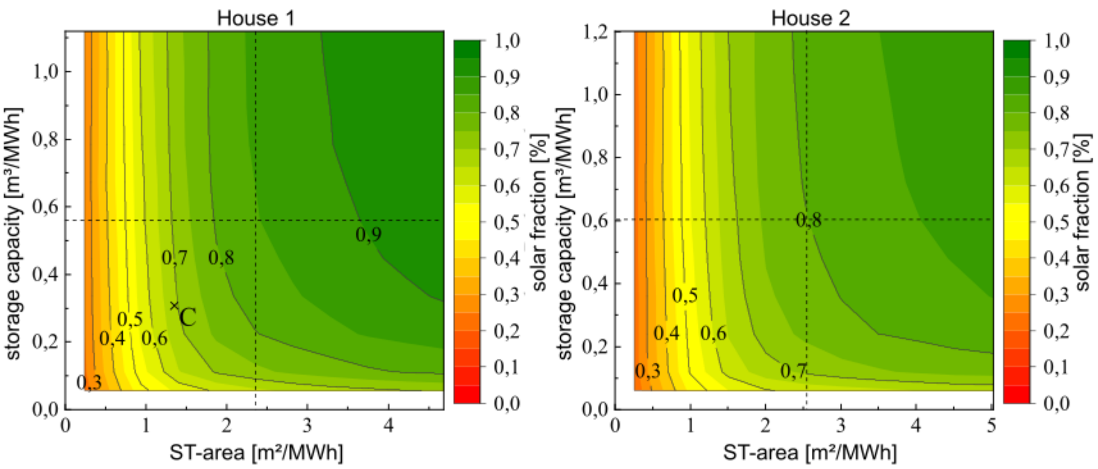

Figure 18 Results of the simulation of the solar fraction of heat normalised to annual heat consumption (heating + DHW), dashed line shows initial situation; C : solar fraction resulting from measured consumption in Cottbus

Figure Figure 19 (left) shows that with an installed capacity of 29.6 kWp (initial situation) per house, the battery is not needed for the power supply at the quaternary level, as almost all the surplus PV yield is generated in the office building. Only from a peak power of more than 95 kWp (0.9 kWp/MWh) in both buildings can be increased by a battery. As the axes in this diagram are normalised to the district electricity consumption (approximately 106 MWh), it is clear that this is approximately a section of the lower left corner of Figure 17. Compared to the analysis of the individual solar houses, only the electricity consumption is increased, while the PV power and battery capacity remain the same.

On the heat supply side, Figure 19 (right) shows that for the realised case in Cottbus, the total volume of the heat storage tanks of around 50 m³ with an ST area of around 200 m² is slightly too large.

The solar fraction of the district would only be reduced by 2 percentage points to 61%. Reducing the ST area, on the other hand, would lead to significant losses in solar fraction.

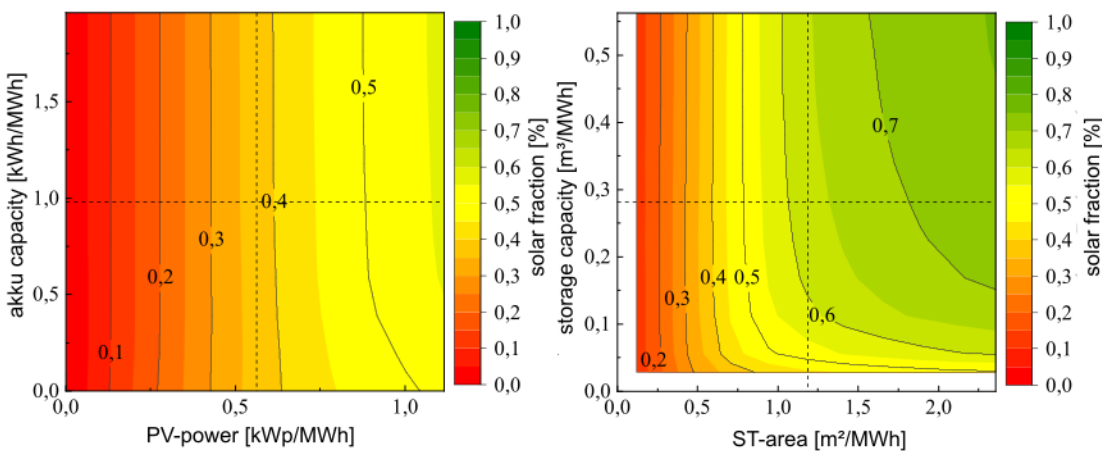

Figure 19 Solar fraction at the district level as a function of the PV power and battery capacity installed in the district or ST area and heat storage volume.

5.2.3.2 Influence of the location

To evaluate the selected sites, a comparison of ST and PV yields is made, as well as a comparison of thermal and electricity consumption. Relevant indicators are also calculated and presented.

On average, the PV and ST yields are highest in Munich and lowest in Hamburg. Compared to the reference site of Cottbus, Hamburg produces on average 1.72 MWh/a less PV and 2.45 MWh/a less ST. In Munich, on the other hand, 2.07 MWh/a (PV) and 1.99 MWh/a (ST) more are produced. The differences are thus up to 16%. The main reason for the differences in yields is the difference in the global irradiance depending on the location.

Cottbus has the highest heat demand at 36.13 MWh/a. It is 1.32 MWh/a higher than in Hamburg and 2.4 MWh/a higher than in Munich. Electricity consumption is almost identical in all simulations as the same user profiles are used. The small deviations of up to 70 kWh/a are due to differences in the provision of auxiliary energy, e.g. for the gas boiler.

The relevant key figures are shown in Figure 20. The solar fractions are highest in Munich and lowest in Hamburg. The differences are less than 10 percentage points in all cases.

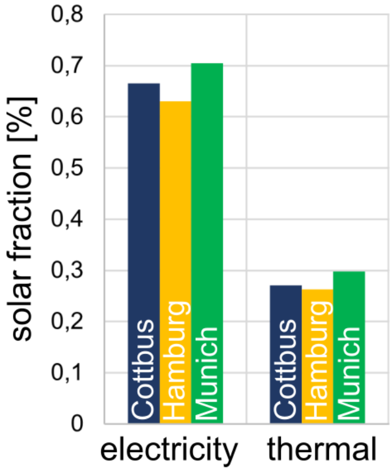

Figure 20 Solar fraction for the electrical and thermal system for the simulation model of the Cottbus houses at the Cottbus, Hamburg and Munich sites

5.2.4 Conclusion - Outcomes

Outcome of the variants for reaching SEB:

- Increasing PV area and battery size would increase solar fraction
- From an economic point of view, the PV area/capacity is currently well chosen. The battery capacity could possibly be reduced slightly in other locations without a major loss of solar fraction.
- For the heat supply, it is clear that increasing the size of the storage tank would not improve the situation; it could be reduced to some extent without significantly changing the solar fraction.
- Even when considering the whole quaternary, it would be possible to reduce the size of the heat storage tank without changing the solar fraction by more than 2%.
- For the electricity side of the quarter, an increase in PV power would have a positive effect on the solar fraction in particular.
- The location in Germany has only a minor influence on the solar fraction of the solar multi-family houses, the concept works almost the same in the locations considered.

5.2.5 References

L. Oppelt, T. Storch, A. Gäbler, T. Fieback: Monitoring results of the energy consumption behaviour of two highly solar-powered apartment buildings, EuroSun2022 Proceedings, 2023, DOI: 10.18086/eurosun.2022.01.09

Johannes Weniger et al.: Dezentrale Solarstromspeicher für die Energiewende. 1st edition. Berlin: Berliner Wissenschafts-Verlag, 2015. isbn: 978-3-8305-3548-5. url:https://pvspeicher.htw-berlin.de/solarspeicherstudie/.

5.3 District with multi-family houses, cold district heating network, ice store and solar thermal air-brine collectors, continental climate (Germany)

Beginning with a summary of the characteristics of the supplied district in chapter 5.3.1 a short description of the implemented control strategy in chapter 5.3.2 and the simulated parameter variations in chapter 5.3.3 conclude this investigation of a district with multi-family houses and a cold district heating network.

5.3.1 District characteristics

In the following, the characteristics of the supplied district are shown. One major characterizing aspect of this district is the cold district heating network connecting the decentral multi-family houses and the installed heat pumps in those houses with the centrally positioned heat sources. Those heat sources are the solar thermal air-brine collectors and an ice store, which is used as a seasonal thermal energy store and as a heat source.

Table 7: District characteristics for a district with multi-family houses and a cold district heating network

District characteristics		
Location	Ludwigsburg (Germany)	
Buildings	9 multi-family houses + one kindergarten with 3 residential units above	
Energy ref. area	8,567 m² (Heated floor area)	
Heating demand (Only space heating, without domestic hot water)	59.3 kWh/(m²a)	
Cooling demand	19.5 kWh/(m²a)	
Heating generator	10 Decentral brine-water heat pumps	
PV	Total area Number of modules Module efficiency (Standard test conditions) Peak power	1,086 m² 595 modules on the roofs 19.46 % 220.15 kW_p
Solar thermal	Total area Number of collectors Peak power per collector Under following conditions: Beam radiation: 850 W/m² Diffuse radiation: 150 W/m² Temperature difference between mean fluid temperature and ambient temperature $(\vartheta_{fluid} - \vartheta_{ambient})$: 0 K -5 K Collector type	137 m² 38 collectors on a roof 1.206 kW_p 3.196 kW_p Solar thermal air-brine collectors
Seasonal thermal energy store	Kind Thermal capacity	Ice store 75.6 MWh
Decentral thermal energy stores	Kind Volume	Hot water stores 9 x 887 l 4 x 1,103 l 2 x 1,500 l
Heating system	Floor heating system	
DHW preparation	Electric instantaneous water heaters	
Cooling system	Active cooling of the whole cold district heating network with one centrally positioned heat pump in one of the 10 buildings Natural cooling by using the ice store as heat sink	

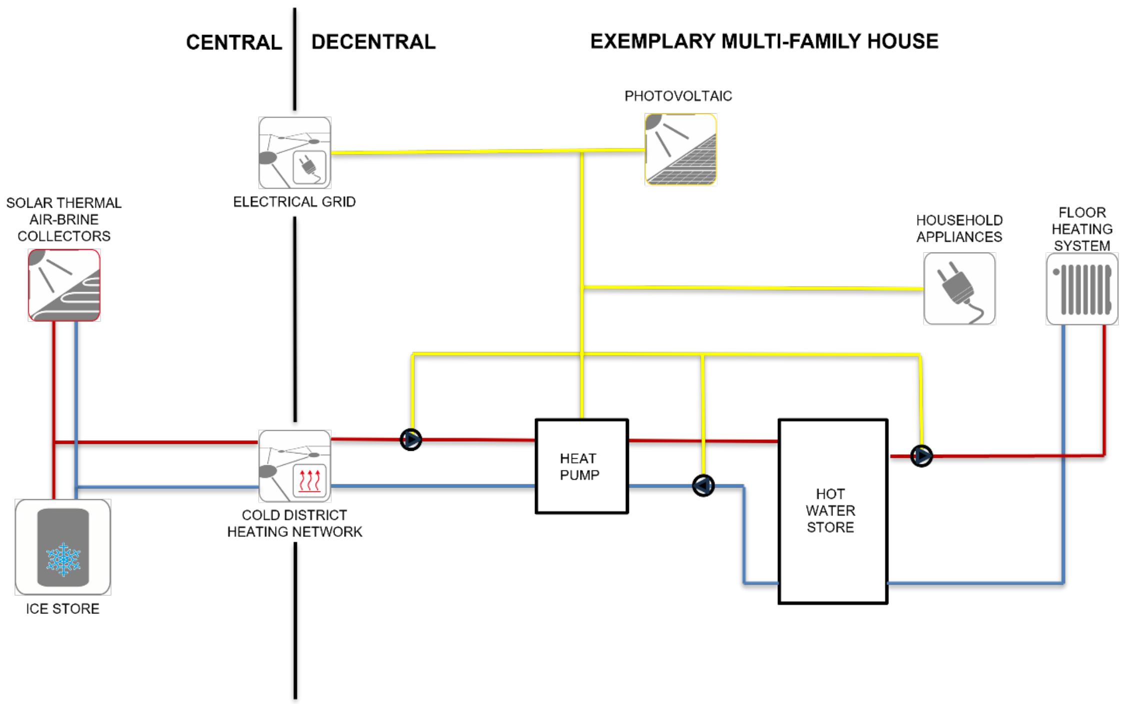

Figure 21: Schematic set-up of the district with one exemplary multi-family house, the cold district heating network, the solar thermal air-brine collectors and the ice store

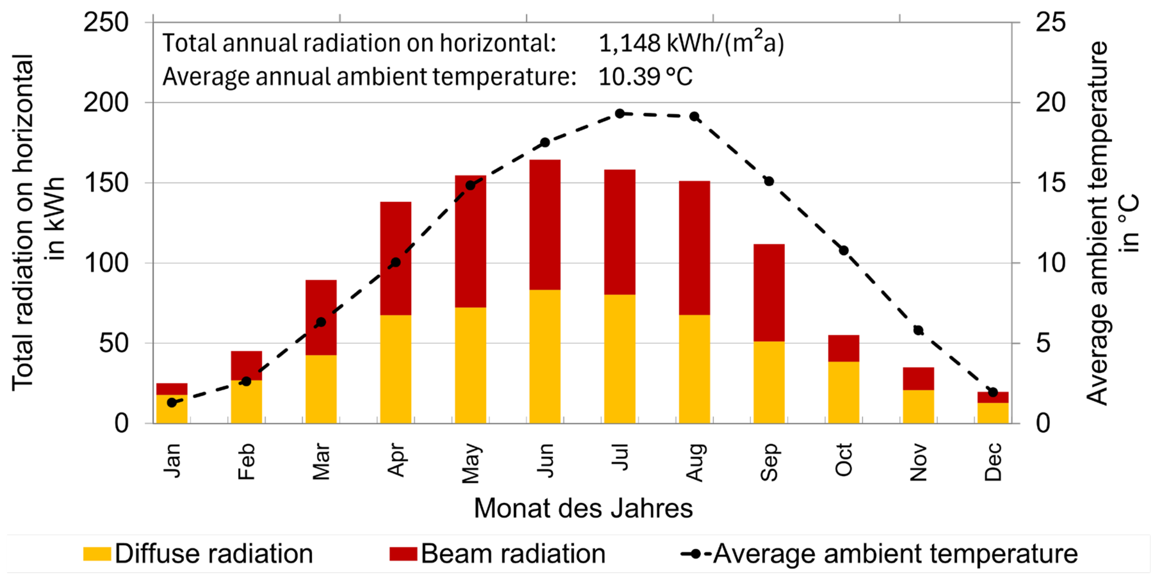

Figure 22: Weather data for Ludwigsburg (Germany) (Source: Test reference year 2017 by "Deutscher Wetterdienst")

5.3.2 System heat management philosophy and control strategy

As mentioned before, the ten multi-family houses are heated by individual heat pumps installed in those houses. The solar thermal air-brine collectors and the ice store are used as heat source and are connected through the cold district heating network with the heat pumps. By default, solar heat gains are used as prioritized heat source. Only if there are no solar heat gains available due to the current weather conditions the ice store is used as heat source. Additionally, the control is programed to continuously discharge the ice store until the end of the heating season to provide capacity in the ice store for cooling purposes in summer.

In the cooling season by default the ice store is used as heat sink. In case the ice store reaches its maximum capacity at a water temperature of about 20 °C one heat pump in one of the ten buildings in the district is designed to actively cool the whole cold district heating network and thereby the ten buildings. This heat pump uses the solar thermal air-brine collectors as heat sink.

In Addition, this heat pump can also be used to actively precool the ice store in summer during nights. This decreases the water temperature in the ice store and thereby provides additional capacity for cooling purposes during the day. This method is more efficient compared to operating the heat pump during the day as the ambient temperatures during the night are lower and therefore the heat pumps efficiency increases.

The electricity produced by the PV modules is either directly used for the heat pumps or transferred to the grid.

The domestic hot water is supplied by electric instantaneous heaters.

5.3.3 Parameter variations

Due to the essential role of the ice store in this cold district heating system as a seasonal thermal energy store the following simulated parameter variations vary the relation between the heating demand and the ice store's thermal capacity. This relation is defined as parameter R.

$$R = \frac{Heating\ demand\ \left[\frac{MWh}{a}\right]}{Ice\ store's\ thermal\ capacity\ [MWh]}$$

In the real district as described in the chapters before the R-value is 6.9 1/a. As the heating demand supplied by the simulation model is only 500 MWh/a instead of 520 MWh/a the R-value of the variant representing the real district is 6.6 1/a. Besides this variant two additional variants with an R-value of 3.3 1/a and 1.7 1/a are investigated. Those lower R-values are reached through decreasing the heating demand compared to the heating demand of the real district. In addition, the cooling demand is also decreased by the same factor as the heating demand.

In Figure 23 the state of charge (SoC) of the ice store for the different parameter variations of the R-value are shown. The state of charge is defined as 100 % for a state with only liquid water and a water temperature of 0 °C in the ice store. With an increasing share of solid water or respectively ice, the state of charge is continuously decreasing below 100 %. Theoretically, at a state of charge of 0 % all liquid water would be solid ice. But the ice store is operated only until around a state of charge of 20 %, as with an increasing ice layer around the pipes of the heat exchanger the efficiency of the heat transfer is decreasing. Additionally, a completely frozen ice store would result in tensions in the material of the storage wall as ice has a higher volume than liquid water. With a rising water temperature above 0 °C the state of charge can increase above 100 % until the water reaches the maximum temperature of 20 °C. This maximum temperature is due to avoid material fatigue in the storage walls.

To provide sufficient capacity both for heating and cooling demands the control limits the extraction of heat and the regeneration, this means the insertion of heat, of the ice store. This is configured by the definition of an extraction and a regeneration limit, which are also shown in Figure 23. The extraction limit sets the limit for the active extraction of heat by the heat pump for cooling purposes in summer. This is necessary to have an ice store with a preferably high SoC at the beginning of the heating season. While the regeneration limit restricts regeneration in the heating season to have a preferably low SoC at the beginning of the cooling season.

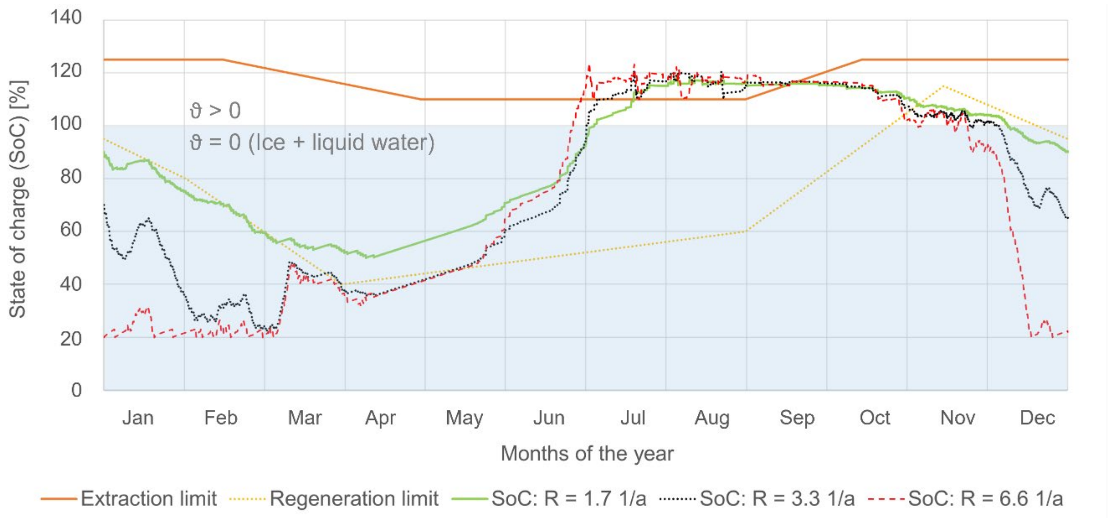

Figure 23: Parameter variation of the R-value (Relation between heating demand and capacity of the ice store)

In the months with heating demand from October until April it can be seen that in all variants heat is extracted from the ice store to be used for heating purposes by the heat pumps. Therefore, the ice fraction is increasing causing the state of charge to decrease in those months while the temperature of the water stays constantly at about 0 °C. By comparing the three variants it can be seen that with increasing heating demand and therefore higher R-value the state of charge is decreasing faster. In case of the variant with an R-value of 6.6 1/a the ice store already reaches its minimal state of charge of about 20 % in December. This results in lower efficiencies of the heat pumps as they are operated with heat with a lower temperature level provided by the solar thermal air-brine collectors. With a lower heating demand in the variant with an R-value of 3.3 1/a the state of charge reaches its minimum only in March. Therefore, the capacity of the ice store in this case with half of the original heating demand is sufficient so that the ice store can be used as a heat source almost during the whole heating season. With an even lower heating demand in the variant with an R-value of 1.7 1/a the state of charge does not reach its minimum of 20 % at any time during the year and therefore the ice store's capacity could be considered too large measuring against the quarter of the original heating demand. To conclude, these simulation results in the heating season led to the assumption that the ice store in the real district should has been designed with a larger capacity. Although, there are more aspects to be considered and might have influenced the chosen ice store's capacity. For example, the local available space or limited investment costs for the ice store.

The state of charge in the variants with an R-value of 3.3 1/a and 6.6 1/a is automatically below the regeneration limit in December, January and February, as the heating demand is high enough. The state of charge of the variant with an R-value of 1.7 1/a is increasing according to the regeneration limit continuously during January and February as the heating demand is low enough. In March the heating demand in this variant is too low to discharge the ice store sufficiently and keep the state of charge below the regeneration limit. Although this results in a lower capacity for cooling purposes in summer this does not lead to negative effects in summer due to the lower cooling demands in this variant.

Beginning in April the heat transferred into the ice store for cooling purposes results in an increasing state of charge in all variants. Furthermore, the variant with an R-value of 6.6 1/a reach the ice store's maximum capacity at a water temperature of about 20 °C and a state of charge of about 120 % at the beginning of July, while the variant with an R-value of 3.3 1/a reaches the same state later in July due to the lower cooling demand.

To decrease the state of charge again during the cooling season one heat pump is used to actively precool the ice store by night. Due to the definition of the extraction limit this cooling – or extraction of heat – is limited to a state of charge of about 110 % to maintain a sufficient capacity for the heating purposes in the following heating season.

In Addition, the seasonal performance factors (SPF) of the three investigated variants can be seen in

Table 8. In the following the definition of the seasonal performance factor is given.

$$SPF = \frac{Useful\ heat\ supplied\ by\ the\ heat\ pumps\ [MWh]}{Electric\ energy\ consumed\ by\ the\ heat\ pumps\ [MWh]}$$

Table 8: Seasonal performance factors (SPF) of the heat pumps in the three investigated variants

	Seasonal performance factor (SPF)
Variant with R = 1.7 1/a	4.72
Variant with R = 3.3 1/a	4.98
Variant with R = 6.6 1/a	4.91

The reason for the lower SPF of the heat pumps in the variant with an R-value of 1.7 1/a compared to the variant with an R-value of 6.6 1/a is that the designed power of the heat pumps has not been reduced according to the increases heating and cooling demands. This is also the case in the variant with an R-value of 3.3 1/a but here the increased efficiency of the heat pumps due to the availability of the ice store as heat source over the whole heating season overcompensates the lower efficiency due to the inappropriate designed power of the heat pumps. In Addition, the difference between designed power and heating and cooling demands is not as large as it is in the variant with an R-value of 1.7 1/a.

5.3.4 Conclusion

In conclusion, this simulation study showed the influence of the heating demand and the thermal capacity of the ice store on the state of charge of the ice store and the seasonal performance factor (SPF) in the period of one year. Especially in the heating season an ice store with a sufficient capacity regarding the actual heating demand can be available as heat source for the heat pumps almost the whole period of the heating season and therefore increases the SPF. In the cooling season in every simulated variant a precooling of the ice store during nights is necessary to use the ice store as heat sink for cooling purposes during the day.

In context of reaching high solar fractions in buildings an ice store functioning as seasonal thermal energy store can store surplus solar heat gains, which can be extracted for heating purposes in periods without available solar heat gains. Therefore, using an ice store – or generally a seasonal thermal energy store – increases the annual solar fraction of the supplied buildings.

5.3.5 References

Drück, H. et al., 2024. Final report of the research project “Development of integrated solar supply concepts for climate-neutral buildings for the “city of the future” (Sol4City)”, Institute for Building Energetics, Thermotechnology and Energy Storage (IGTE), University of Stuttgart, Stuttgart. (Publication expected in late 2024)

Deutscher Wetterdienst (DWD), 2017. Ortsgenaue Testreferenzjahre von Deutschland für mittlere, extreme und zukünftige Witterungsverhältnisse, Offenbach.

5.4 Two multi-family houses, moderate climate (Austria)

5.4.1 Building and System

Table 9 shows building and system data used as the starting point of the simulations and study. In chapter 5.4.3 all variants are listed.

The complete simulation study is presented in the Journal Paper (Ochs, Franzoi, Dermentzis, Monteleone, & Magni, 2023). The results presented in this section provide a summary of the findings from that study.

Table 9: Building and system data for Block of multi-family houses

Building Data	
Location	Innsbruck (Austria)
Building	Two Multi-family Houses
Energy ref. area	2,148.8 m² (TFA) (North building: 1295.6 m², South building: 853.2 m²)
Useful energy (Q_{cons} and E_{cons})	
Heating demand	Design: North building: 11.0 kWh/(m²a), South building: 14.2 kWh/(m²a) Measured: North building: 18.7 kWh/(m²a), South building: 17.1 kWh/(m²a) Measured values are used in the simulations
Cooling demand	- kWh/(m²a) (passive cooling is possible but it is not simulated)
DHW demand	Design: North building: 19.6 kWh/(m²a), South building: 24.5 kWh/(m²a)
Household demand	Appliances: 17.9 kWh/(m²a); Auxiliaries: 8.0 kWh/(m²a)
E-mobility demand	- kWh/(m²a)
Total heating demand	Design: 33.7 kWh/(m²a) Measured: 39.6 kWh/(m²a) Measured values are used in the simulations
Total electricity demand	37.0 kWh/(m²a)
Final energy (Qf)	37.0 kWh/(m²a)

System Data		
Heating generator	Ground-source heat pump (double-staged)	
Colling generator	- (option for passive cooling is disregarded in the simulations)	
PV	Total area	152.3 m²
	Number of modules (placed)	97 modules on the roof
	System efficiency (including all periphery)	11 %
	Peak power	24.5 kWp
Solar thermal	Total area	80 m²
	Total aperture area	73.6 m²
	Thermal capacity	
	Collector type	Flat plate collector
Thermal storage	Volume	1 x 6000 l
Electrical storage	Capacity	-
	Storage type	-
Ventilation system	System	Mechanical ventilation
	Air change	0.3 1/h
	Heat recovery	Yes, efficiency of 81%
Heating system	Floor heating	
DHW preparation	Fresh water station in each flat	
Cooling system	Passive cooling is possible through floor heating (but not simulated)	

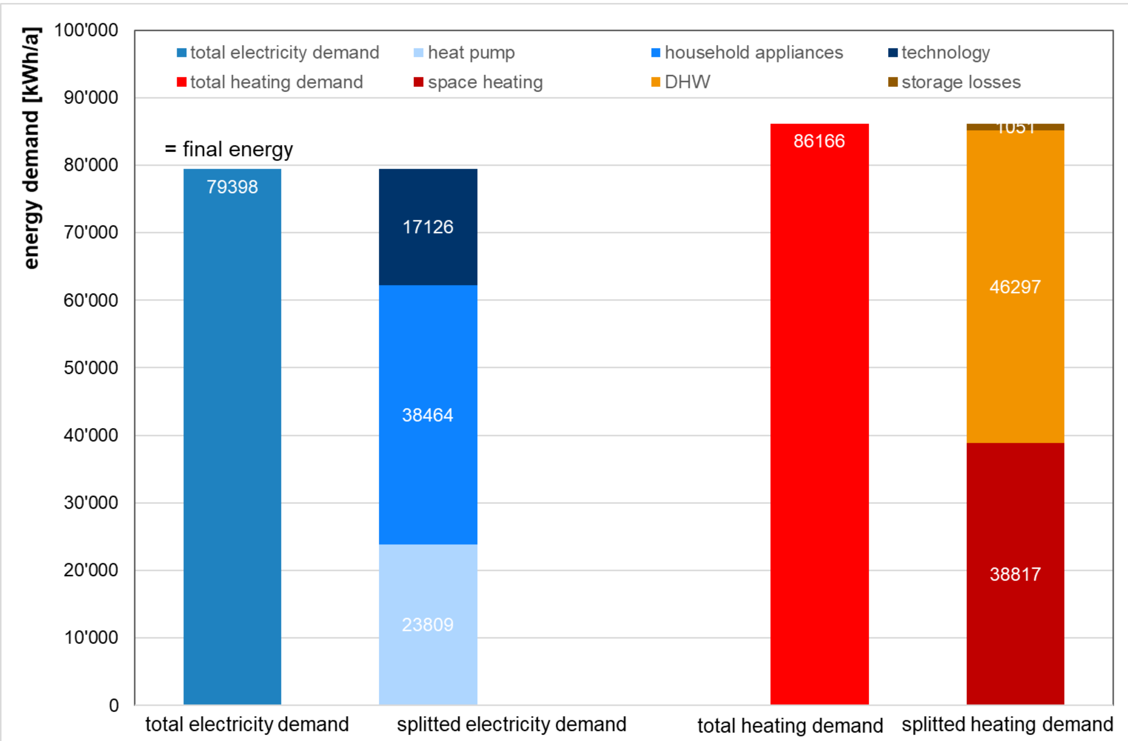

Figure 24: Electricity demand and demand of thermal energy of the building

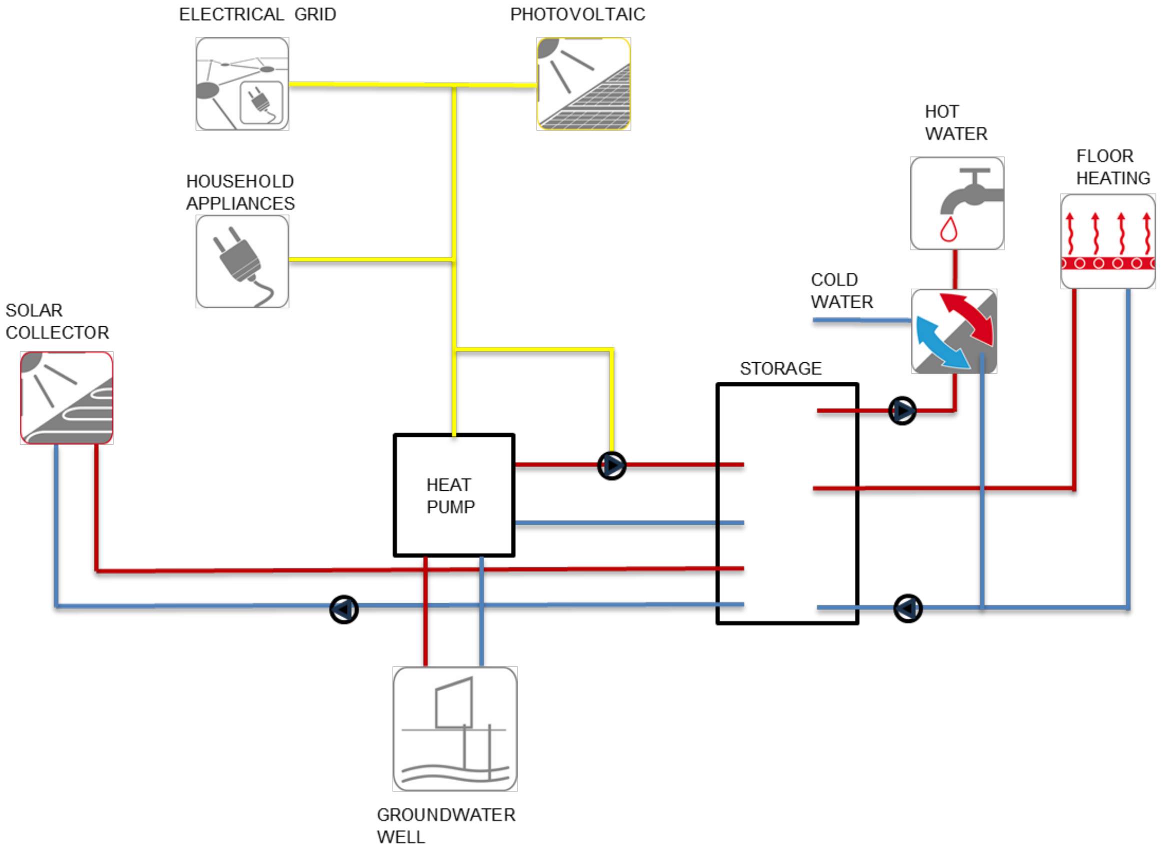

Figure 25: energy concept and systems

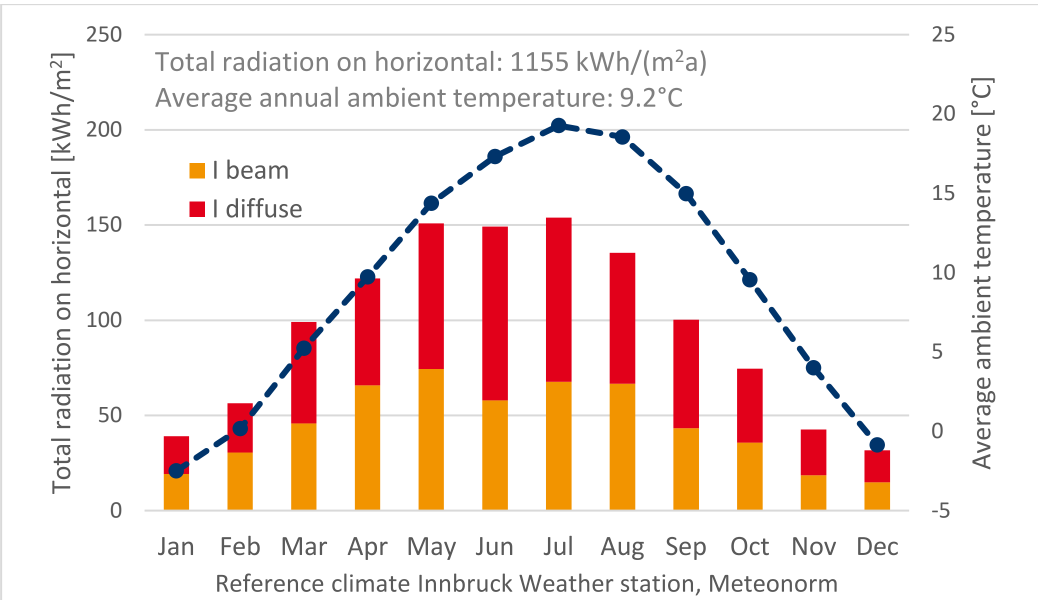

Figure 26: Weather data Innsbruck (Austria), average ambient temperature, and solar radiation on horizontal. Source: **(Meteonorm 8, 2020)**

5.4.2 System management philosophy/control strategy

The multi-family buildings have a very good thermal envelope, meeting the Passive House standard (i.e., with a space heating demand below 15 kWh/(m²a)). Mechanical ventilation units (one in each building) provide hygienic air renewal with minimal energy use, thanks to 81% heat recovery efficiency. A hydronic system supplies space heating (SH) and domestic hot water (DHW) to both buildings using a double-stage groundwater-source heat pump (GWHP) connected to a thermal energy buffer storage (BS). The hydronic system is a 2+2-pipe system, i.e., 2 separate flow pipes for SH and DHW and 2 separate return pipes for SH and DHW. The 2 return pipes are mixed just before entering in the storage. The heat pump includes a de-superheater, which improves efficiency by enabling simultaneous SH and DHW preparation without raising condensation temperature. The heat pump (HP) prioritizes DHW preparation by operating at full power, with both compressors running. In SH mode, typically only one compressor is active, but the second compressor may be activated occasionally to accelerate the storage tank loading process. The roof surfaces of the two buildings are covered by photovoltaic (PV) and solar thermal (ST) panels. The BS stores water for SH and DHW preparation and it is charged by the HP and the ST. The Buffer Storage (BS) uses a configuration known as Combi-storage (Haller, Haberl, Mojic, & Frank, 2014), which combines water at different temperature levels. Ideally, the BS can be divided into three sections: the top stores water for DHW preparation, the middle for SH, and the bottom collects colder return water, serving as extra storage during periods of high ST contribution. System water, not drinking water, is stored, with decentralized DHW heat exchangers (freshwater stations) in each flat for hot water preparation.

5.4.3 Simulation variations

Alternative HVAC system configurations are investigated to further reduce the energy consumption and reach the NZEB goals (see Table 10). The building model has been calibrated on the monitoring data so that the space heating demand corresponds to the monitored space heating consumption. One variant explors the possibility of relying solely on onsite electricity generation, replacing ST with photovoltaic (PV) panels, covering the entire roof and allowing for a smaller buffer storage, since the excess PV electricity is fed back into the grid. Two variants focus on reducing the thermal storage to serve only DHW preparation, with two alternative system layouts. In one layout, a single-stage HP is connected directly to the SH loop (reducing the number of circulation pumps required). In the second layout, the condenser and desuperheater are connected in series (instead of a parallel connection). These three variants consider the electricity required for SH (including losses), DHW (including losses) and auxiliaries. In the fourth variant, appliances demand is also included in the energy balance.

Table 10: Simulation variants

Variation	Starting point	Changes/ adaptions
PV instead of ST	Reference system (as described in XX**Fehler! Verweisquelle konnte nicht gefunden werden.**)	PV panels instead of ST
BS only for DHW + system layout “direct SH”	PV instead of ST	• BS connected only to DHW preparation loop • Reduction of the BS size • Single-stage HP without DSH
BS only for DHW + system layout “CND-DSH series connection”	PV instead of ST	• BS connected only to DHW preparation loop • Reduction of the BS size • Condenser and desuperheater in series connection instead of parallel
Including appliances	BS only for DHW + system layout “direct SH”	Appliances (17.9 kWh/(m²a)) included in the energy balance

5.4.4 Results

5.4.4.1 Influence of the PV panels instead of ST panels

Based on the pre-design study results (Ochs, Dermentzis, and Feist 2014), solar thermal collectors were installed to partially cover the domestic hot water (DHW) demand and contribute to space heating (SH) demand. However, the benefits of ST on SH are critical, especially in buildings with very low SH demand. The monthly electricity consumption (including the HP and the auxiliaries) with and without the ST panels is shown in Figure 27. There is a considerable increase in energy consumption during the summer months because of the absence of ST. During the heating season, the increase is limited (between 0.1 kWh/m² and 0.3 kWh/m² in the winter months from November to February). Besides, the PV production is also shown (green lines) for the two cases (with and without ST-replaced by PV).

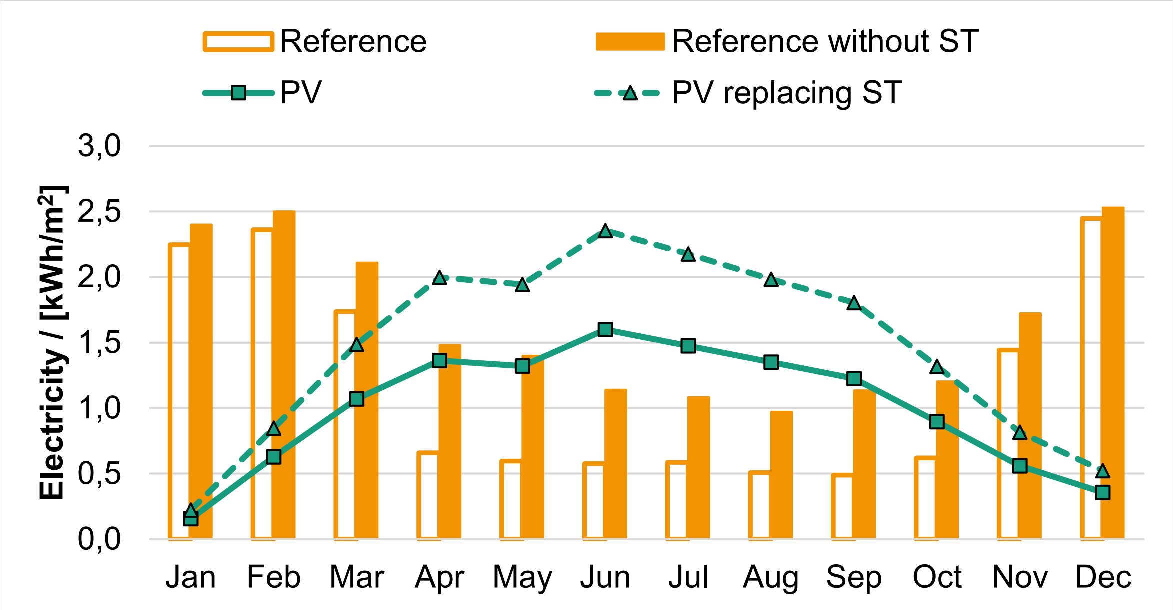

Figure 27: Comparison of monthly electric consumption (of the HP, and auxiliaries) for the reference model and for the case without ST panels. Source: (Ochs, Franzoi, Dermentzis, Monteleone, & Magni, 2023)

Annual values of energy consumption, PV yield and energy balance are shown in Table 11. The use of PV instead of ST slightly improves the energy balance (-2.2 kWh/(m²a) instead of -2.3 kWh/(m²a)). Nevertheless, there is a large surplus of energy generation during the summer months. Moreover, there is room for optimization of the system without ST (e.g., by reducing the size of the thermal storage).

Table 11: Annual electricity consumption, annual PV yield, and annual balance for the reference case, and for the reference without ST but with a larger PV area. Source: (Ochs, Franzoi, Dermentzis, Monteleone, & Magni, 2023)

	Reference	**Reference w/o ST + PV instead of ST**
Annual consumption [kWh/(m²a)]	14.3	19.7
Annual PV yield [kWh/(m²a)]	12.0	17.5
Annual Balance [kWh/(m²a)]	-2.3	-2.2

5.4.4.2 Influence of efficiency and area of solar applications (PV and ST)

When the BS serves only the DHW demand, two systems layouts are considered: one with the single-stage HP ("direct SH") and one with the condenser and desuperheater connected in series instead of the parallel connection ("CND-DSH series connection"), see Figure 28 left and right, respectively.

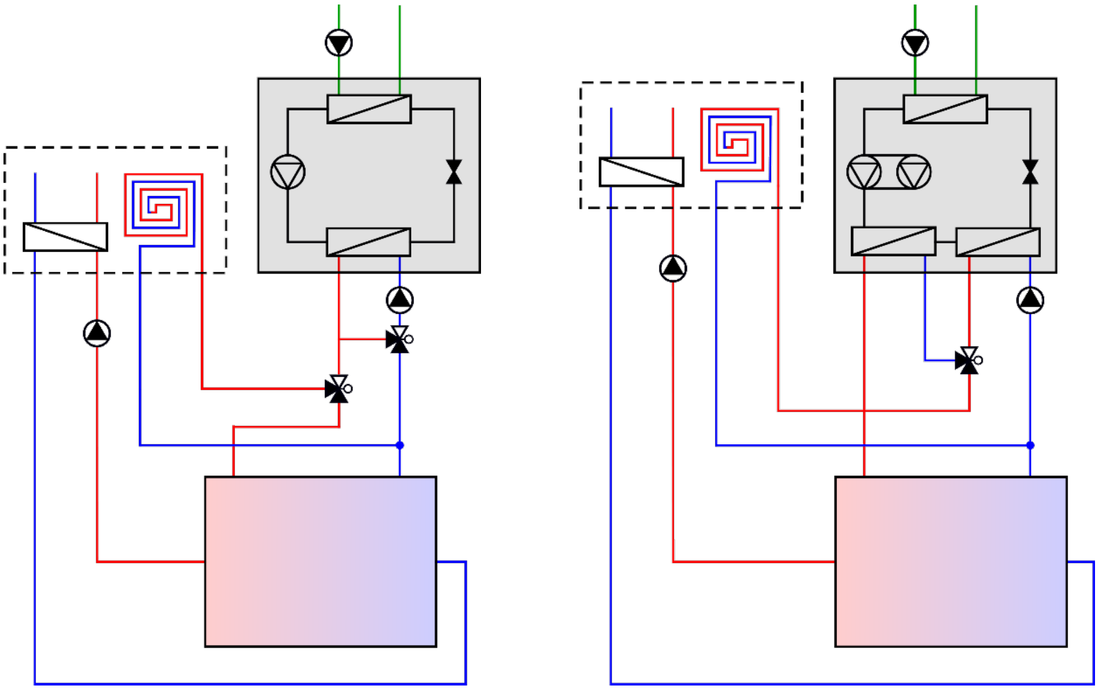

Figure 28: Alternative system design layouts: Case "direct SH" (left) and Case "CND-DSH series connection" (right). Source: (Ochs, Franzoi, Dermentzis, Monteleone, & Magni, 2023)

The energy consumption during the heating season decreases with both system design layouts, whereas, due to the absence of ST, the energy consumption in summer is higher. However, the PV system yield is sufficient to cover this added consumption on a net basis.

The "direct SH" configuration performs slightly better than the "CND-DSH series" one, except for December and January. This is because the contribution of the DSH during the months of peak heating demand is such to reduce the time needed for DHW mode, improving the performance of the HP. Nevertheless, the improvement is negligible and not enough to justify the need for a DSH. Indeed, the DSH is particularly effective in buildings whose heating demand is larger than the DHW demand, which is not often the case in high-performance multi-apartment buildings.

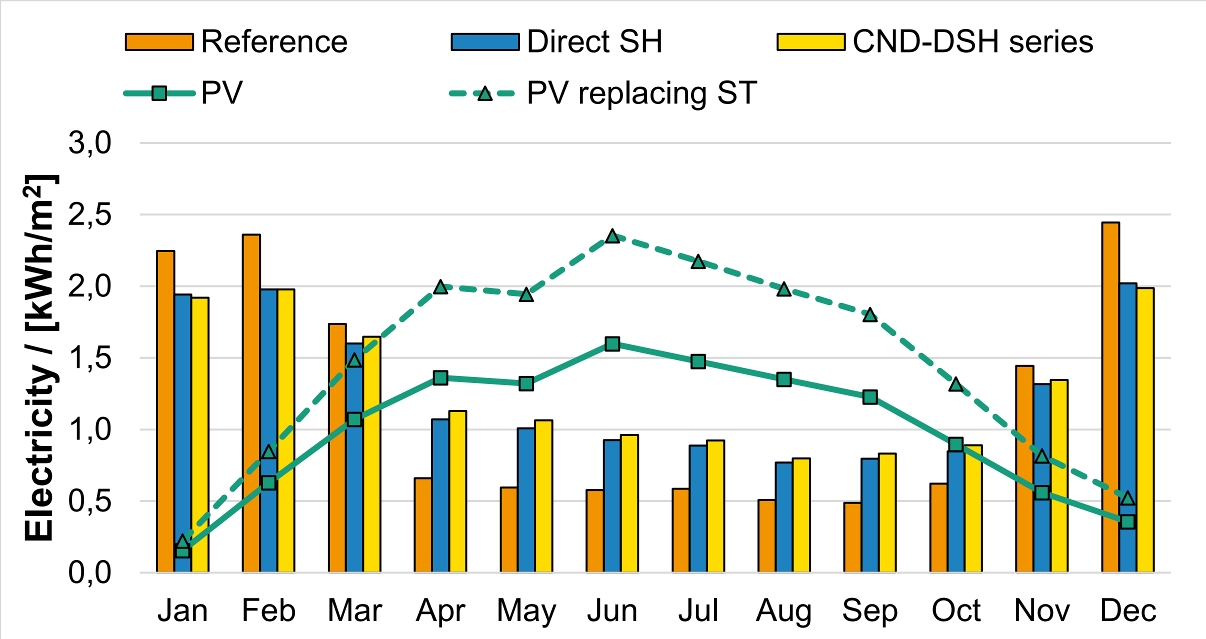

Figure 29: Comparison of total electric consumption (HP and auxiliaries) for Reference case, direct space heating case, and condenser-desuperheater case. Source: (Ochs, Franzoi, Dermentzis, Monteleone, & Magni, 2023)

By increasing the PV system surface to occupy the roof left free by the ST collectors, there is an annual surplus of energy generation as shown in Figure 30. In comparison to the reference case, the alternative system designs, reduce considerably the auxiliary energy consumption. Although the annual total energy consumption of the two alternative systems is increased compared to the reference case, due to the additional PV production the net balance can be reached. This was not the case with the reference system in which some grid electricity is required.

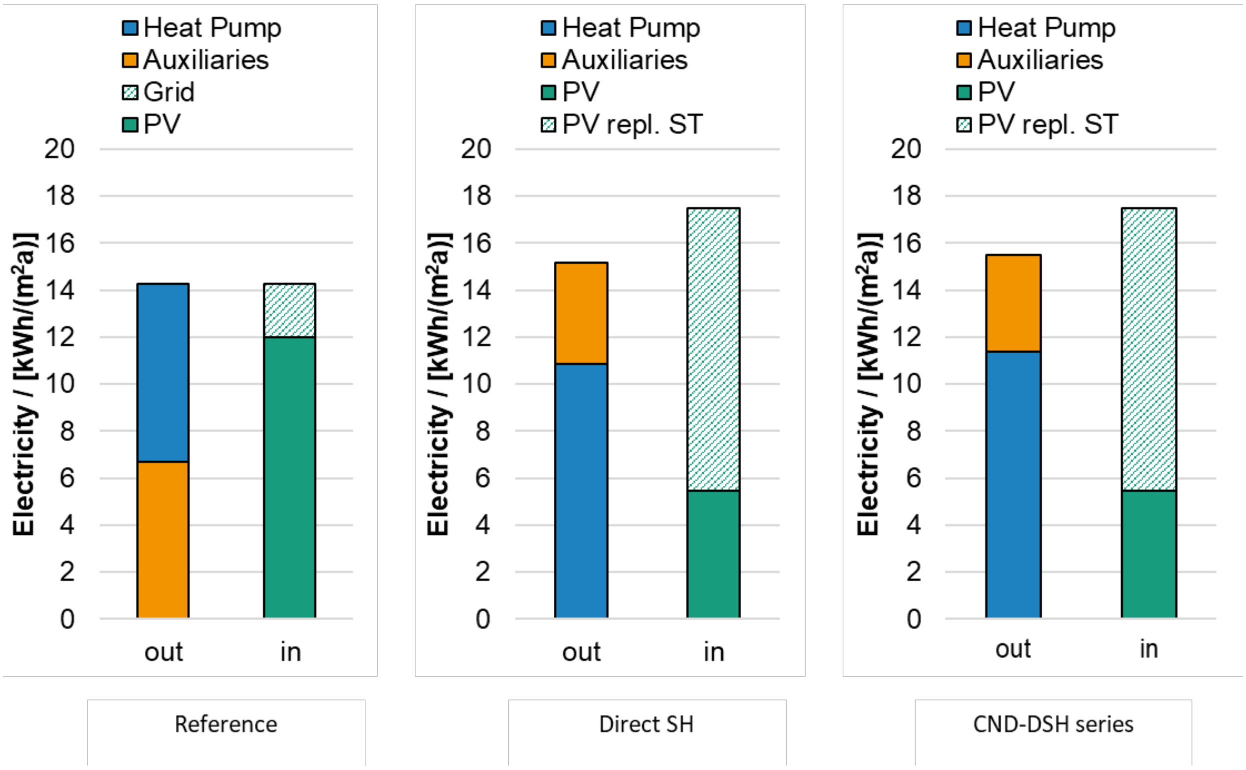

Figure 30: Annual electric energy balance for Reference case (left), direct space heating case (center), and condenser-desuperheater case (right). Source: (Ochs, Franzoi, Dermentzis, Monteleone, & Magni, 2023)

5.4.4.3 Influence of efficiency and area of solar applications (PV and ST)

An energy demand for appliances of 1500 kWh/a per flat is assumed. This is a rather optimistic value, considering the estimated average consumption for Austria of about 3200 kWh/a per flat (Ochs, Magni, Venturi, Tosatto, & Streicher, 2021). The monthly electric energy demand including appliances is shown in Figure 31. In this case, the PV yield is insufficient to meet the monthly electricity demand, particularly during the heating season. This highlights the importance of focusing the design effort on minimizing the energy demand and maximizing the performance of the heating system in the winter months to decrease the dependence on the grid. Additionally, it raises the question of whether optimizing the PV self-consumption control is relevant, given that it could be directly used for household energy needs.

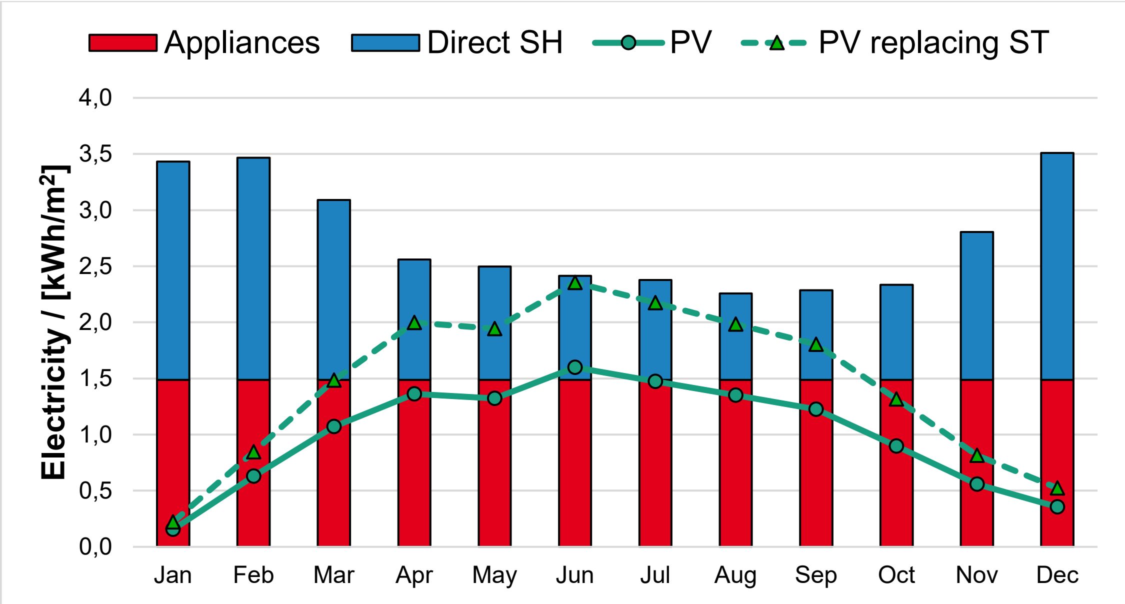

Figure 31: Total monthly electric energy consumption including appliances for the direct space heating case. Source: (Ochs, Franzoi, Dermentzis, Monteleone, & Magni, 2023)

5.4.5 Conclusion – Outcomes

Outcome of the variants for reaching SEB:

- An alternative system design with a separate DHW buffer and direct connection of the HP to the floor heating (or in combination with a small hydraulic separator for the SH loop) is recommended.
- Overall, system simplification is recommended (e.g., PV instead of ST).
- Auxiliary energy should be accounted for in the energy balance, as it makes a significant contribution in low-energy buildings.
- Energy demand for appliances should be accounted for in the energy balance, as it makes a significant contribution, especially in large multi-family buildings. The PV production can be dedicated solely to cover the appliances demand.
- Solar thermal collectors contribute to the reduction of energy needs during the summer. However, PV energy is also able to cover these needs in combination with a heat pump. Both sources have a limited contribution during the winter months, though PV has the advantage of limiting the design complexity. Therefore, for this case study, the presence of both ST and PV is redundant.

5.4.6 References

Haller, M. Y., Haberl, R., Mojic, I., & Frank, E. (2014). Hydraulic Integration and Control of Heat Pump and Combi-storage: Same Components, Big Differences. *Energy Procedia, 48*, 571-580. doi:https://doi.org/10.1016/j.egypro.2014.02.067.

Meteonorm 8. (2020). Meteonorm Version V8.2.0.24079. *Irradiation data for every place on Earth. Globale meterologische Datenbank für Ingenieure, Planer und Ausbildung.* Bern, Switzerland: Meteotest AG.

Ochs, F., Franzoi, N., Dermentzis, G., Monteleone, W., & Magni, M. (2023). Monitoring and simulation-based optimization of two multi-apartment NZEBs with heat pump, solar thermal and PV. *Journal of Building Performance Simulation*.

Ochs, F., Magni, M., Venturi, E., Tosatto, A., & Streicher, W. (2021). Cost-optimal nZEB HVAC configurations with onsite storage. *E3S Web Conferences*, *246.* doi:DOI: 10.1051/e3sconf/202124607001

5.5 Single-family houses, temperate climate (Denmark)

5.5.1 Building and System

Table 12 shows the building and system data used as the starting point of the simulations and study. In chapter 5.5.3 all variants are listed.

Table 12: Building and system data for a single-family house

Building Data		
Location	Copenhagen (Denmark)	
Building	Single-family house	
Energy ref. area	120.4 m^2 (Gross floor area)	
Useful energy (Q_{cons} and E_{cons})	Passive building	Low-energy building
Heating demand	17.4 kWh/(m^{2}a)	55.3 kWh/(m^{2}a)
Cooling demand	0 kWh/(m^{2}a)	0 kWh/(m^{2}a)
DHW demand	21.7 kWh/(m^{2}a)	21.7 kWh/(m^{2}a)
Household demand	29.1 kWh/(m^{2}a)	29.1 kWh/(m^{2}a)
E-mobility demand	0 kWh/(m^{2}a)	0 kWh/(m^{2}a)
Total heating demand	42.6 kWh/(m^{2}a)	78.6 kWh/(m^{2}a)
Total electricity demand	40 kWh/(m^{2}a)	46.4 kWh/(m^{2}a)
System Data		
Heating generator	PVT heat pump	
Colling generator	none	
(PV)T – electrical part	panel efficiency (unglazed) Peak power per panel	21% 0,44 kWp
PV(T) – thermal part	Eta0 bu b1 b2 Collector type	0.55 0 s/m 14.5 W/(m^{2}K) 4.5 Ws/(m^{3}K) Racell PVT unglazed
Thermal storage	Volume	110 l
Electrical storage	Capacity Storage type	- -
Ventilation system	System Air change Heat recovery	Natural ventilation 0.45/h 0 %
Heating system	Floor heating	
DHW preparation	Domestic hot water tank	
Cooling system	none	

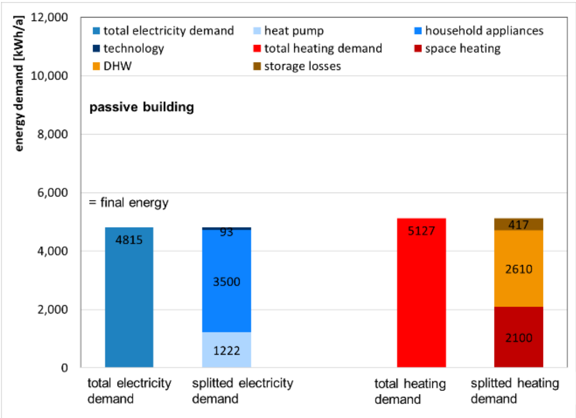

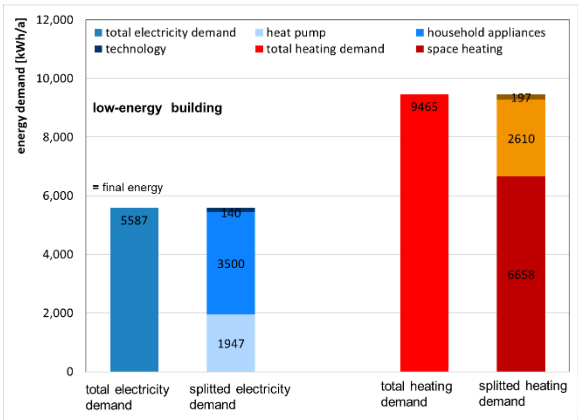

Figure 32: Electricity demand and demand of thermal energy of the passive building (left) and low-energy building (right)

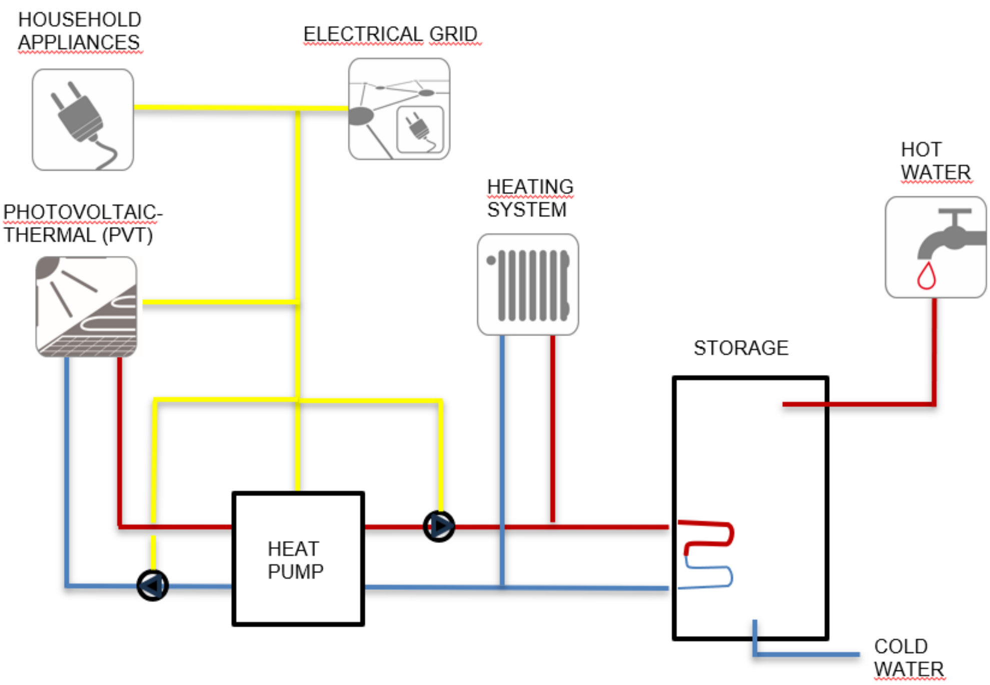

Figure 33: energy concept and systems

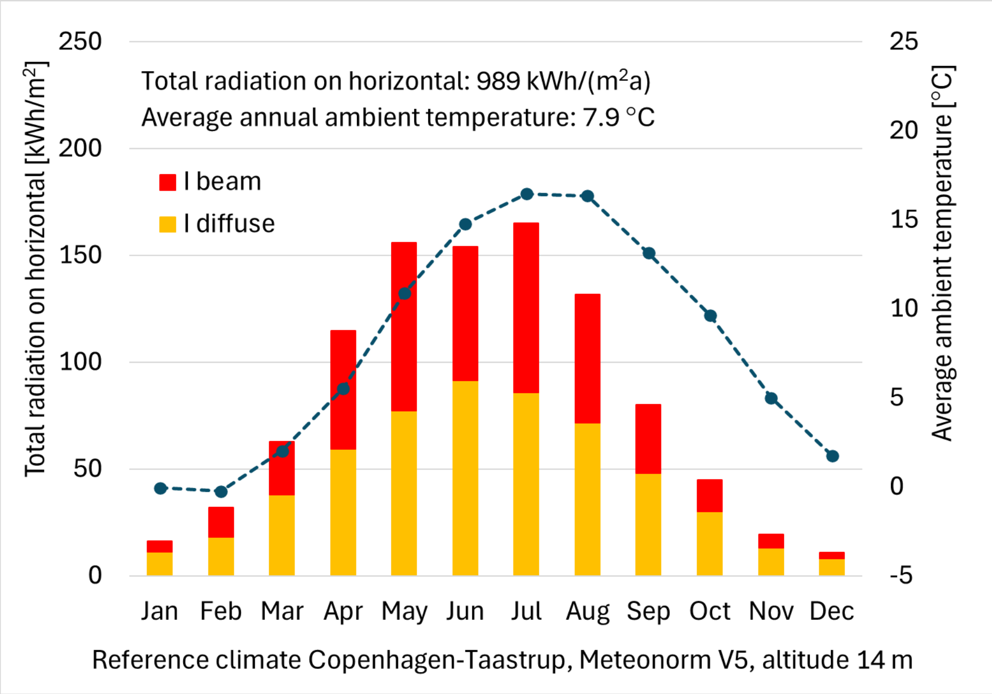

Figure 34: Weather data Copenhagen-Taastrup (Denmark), average ambient temperature and solar radiation on horizontal

5.5.2 System heat management philosophy/control strategy

The heat supply is provided by a brine-to-water heat pump. The energy for the heat pump evaporator is delivered solely from the thermal part of the PVT panel, which draws energy from the solar radiation and ambient air. The heat pump operates the heating circuit in a low temperature range (underfloor heating) and provides domestic hot water for the bathroom and kitchen via the heat storage. The ventilation of the building is performed by natural ventilation (0.3 l/s/m^2). The electric part of the PVT panel provides support to the power supply. The remaining electricity required for household and technical purposes is drawn from the public grid. Domestic hot water has priority over space heating.

As soon as the PVT system produces electricity, it is allocated as follows / in the following order:

1. household appliances
2. heat pump (compressor)
3. system technology (e.g., circulation pumps)
4. Battery storage (if available)
5. grid feed-in

5.5.3 Simulation variations

The simulation variations are listed in Table 13.

Table 13: Simulation variants

Variation	Starting point	Changes/ adaptions
thermal building standard	no changes apart from insulation	"good“ = low-energy house – 30 kWh/(m²a) "very good” = passive house – 15 kWh/(m²a)
tilt of PVT panel	building orientation south	0°, 15°, 30°, 45°, 60°, 75° and 90°
area of PVT panel	building orientation south	10 m^2, 20 m^2, 30 m^2, 40 m^2 and 50 m^2
Battery storage	Battery included in both building types (passive and low-energy)	“small” = 10 kWh “large” = 30 kWh

5.5.4 Results

5.5.4.1 Influence of thermal insulation of the building, PVT panel area, and tilt

The results are shown as electrical solar fraction (f_sol,el) and supply cover factor (SCF_{PV}). The electrical solar fraction increases with increasing area of the PVT panel while the supply cover factor decreases because the ability to utilize one's own produced electricity decreases, and an increasing share of the electricity is exported to the public grid. The thermal solar fraction (f_sol,th) is not relevant in this specific PVT/heat pump system design since the solar thermal energy is solely used to operate the heat pump.

5.5.4.1.1 PVT/heat pump system without battery storage

The electrical solar fraction peaks for PVT tilts between 15° and 60° for small PVT areas (<20 m^2), and for PVT tilts from the 0°-30° for larger PVT areas (>20 m^2).

The supply cover factor is highest for PVTs with a tilt of 0° or 90°. For these tilts, the energy demand is relatively high in the hours where the PVT panels produce energy. For other south facing tilts, a relatively large part of the energy production from the PVT panels cannot be used directly to cover the energy demand in the house.

The results are not influenced by the insulation degree of the building.

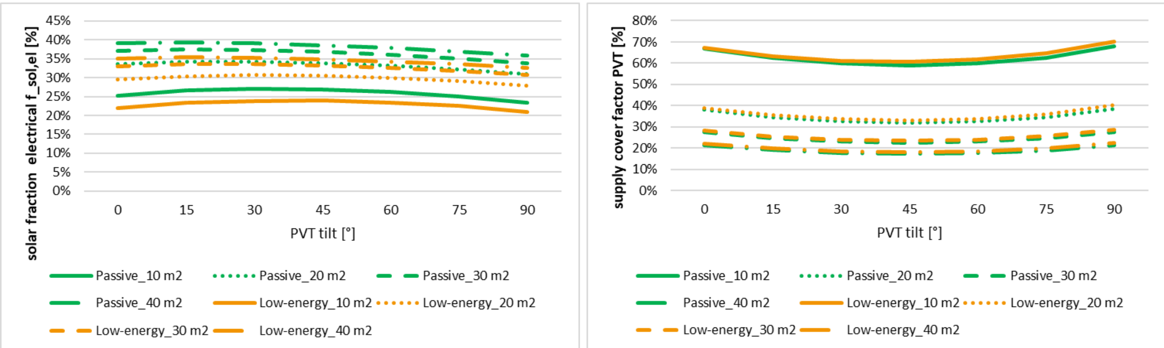

Figure 35: Solar fraction (left) and supply cover factor (right) for differently sized and tilted PVT systems

5.5.4.1.2 PVT/heat pump system with 10-kWh and 30-kWh battery storage

The electrical solar fraction peaks for PVT tilts between 30° and 60° for small PVT areas (<20 m^2), and for PVT tilts from the 30°-90° for larger PVT areas (>20 m^2).

For small PVT areas (<10 m^2), the supply cover factor is 100% regardless of the PVT tilt. For larger PVT areas (>20 m^2), the supply cover factor is highest for PVTs with a tilt of 90°.

The results are not influenced by the insulation degree of the building.

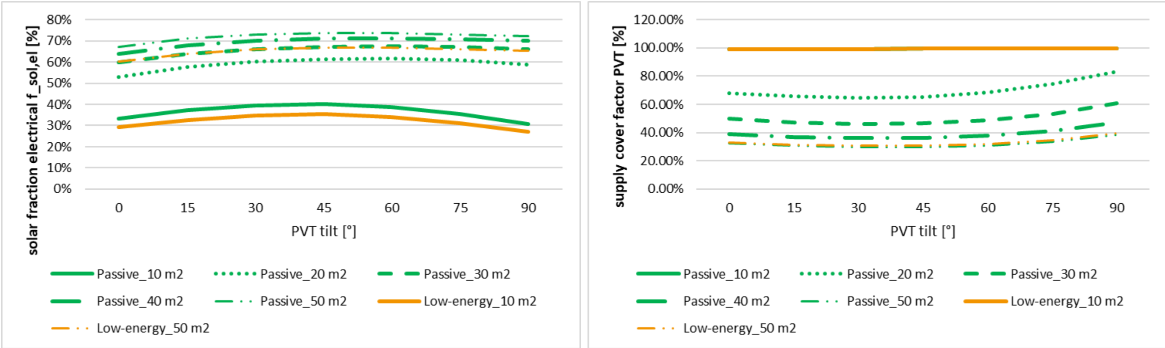

Figure 36: Solar fraction (left) and supply cover factor (right) for differently sized and tilted PVT systems with a 10 kWh battery

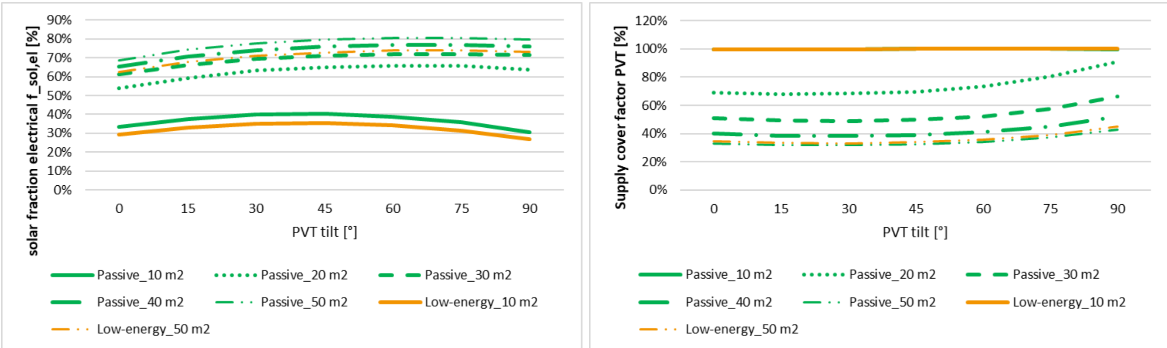

Figure 37: Solar fraction (left) and supply cover factor (right) for differently sized and tilted PVT systems with a 30 kWh battery

5.5.4.2 Energy production, feed-in, and electricity purchase from the local grid

5.5.4.2.1 PVT/heat pump system without battery storage

The optimal tilt for producing the highest electrical output from the PVT is about 45°.

The thermal output from the PVT is hardly influenced by the PVT area and tilt as the thermal output solely depends on the heat demand of the house/the heat pump operation.

The electricity supply to the grid increases for increasing PVT area, and most electricity is exported to the public grid for a PVT tilt of 45° because this is the optimal tilt for maximizing the solar irradiance on the PVT in the Danish climate.

The amount of energy drawn from the grid decreases as the PVT area increases.

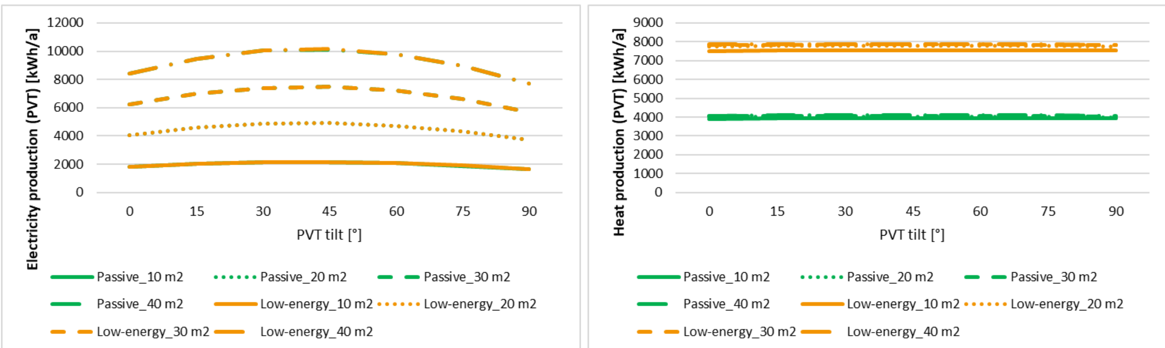

Figure 38: Electricity production (left) and heat production (right) for *differently sized and tilted PVT systems*

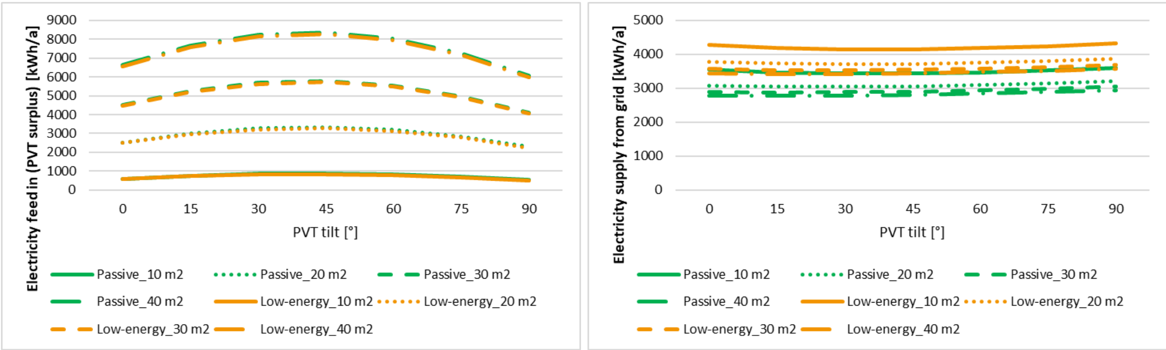

Figure 39: Electricity feed in (left) and electricity supply from grid (right) for *differently sized and tilted PVT systems*

5.5.4.2.2 PVT/heat pump system with 10-kWh and 30-kWh battery storage

The optimal tilt for producing the highest electrical output from the PVT is about 45°.

The thermal output from the PVT is hardly influenced by the PVT area and tilt as the thermal output solely depends on the heat demand of the house/the heat pump operation.

The electricity supply to the grid increases for increasing PVT area, and most electricity is exported to the public grid for a PVT tilt of 45° because this is the optimal tilt for maximizing the solar irradiance on the PVT in the Danish climate.

The amount of energy drawn from the grid decreases as the PVT area and battery storage capacity increases

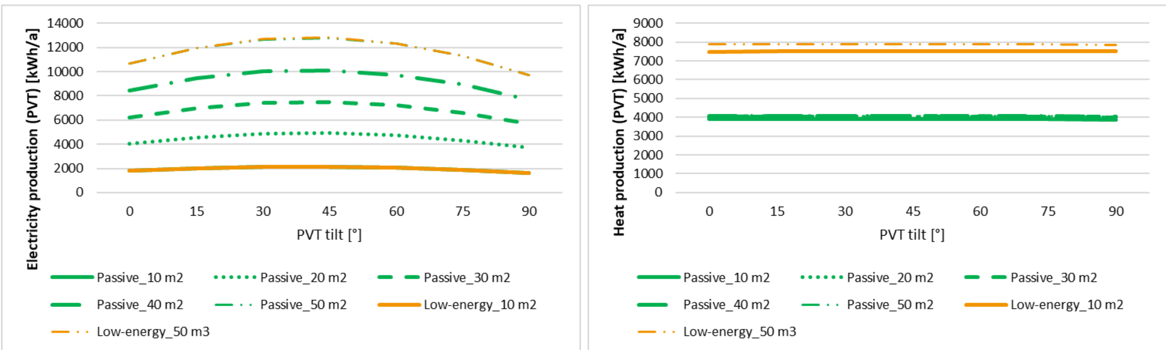

Figure 40: Electricity production (left) and heat production (right) for *differently sized and tilted PVT systems with a 10 kWh battery*

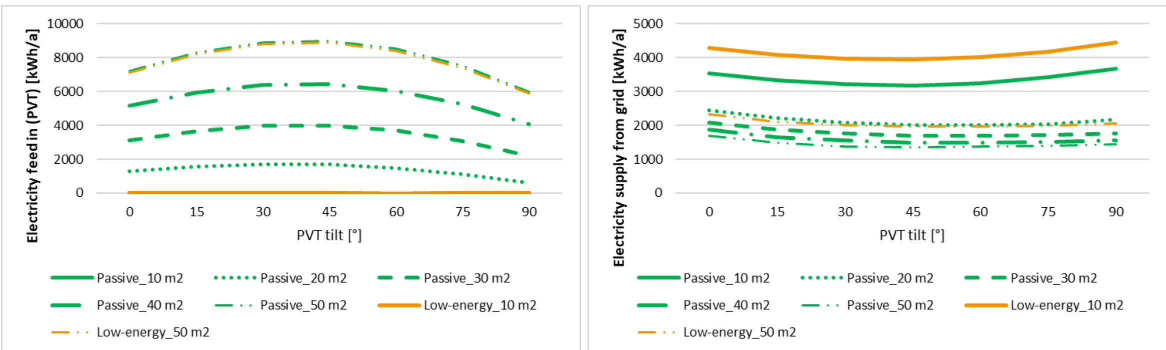

Figure 41: Electricity feed in (left) and electricity supply from grid (right) for *differently sized and tilted PVT systems with a 10 kWh battery*

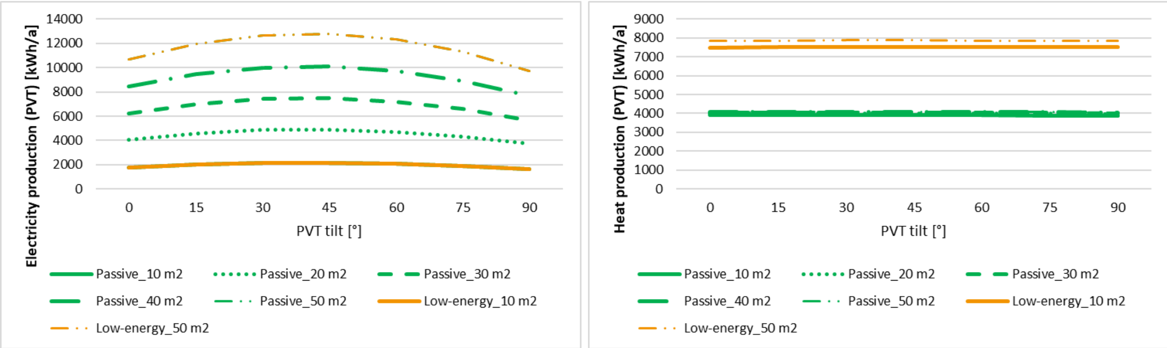

Figure 42: Electricity production (left) and heat production (right) for *differently sized and tilted PVT systems with a 30 kWh battery*

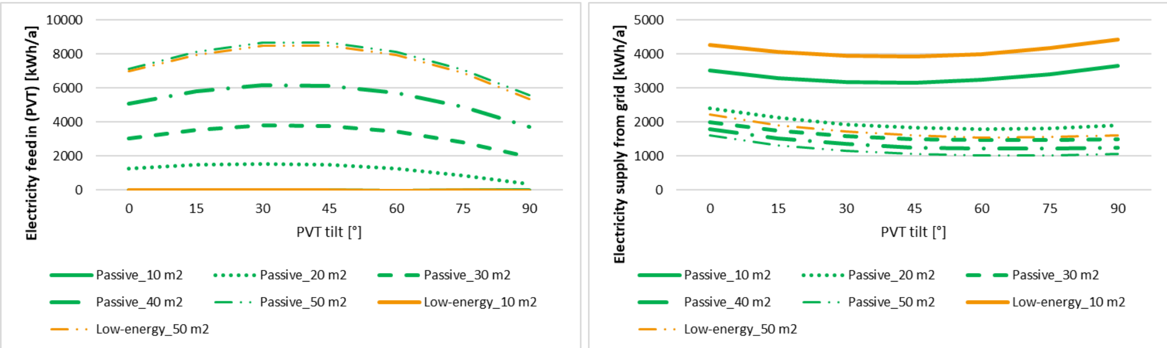

Figure 43: Electricity feed in (left) and electricity supply from grid (right) for *differently sized and tilted PVT systems with a 30 kWh battery*

5.5.5 Conclusion - Outcomes

Outcome of the variants for reaching SEB:

- High electrical solar fractions can only be achieved by including a battery storage for storing the electricity for later use
- In the passive house, electric solar fractions of up to 40% can be reached with a PVT area of 40 m², while electric solar fractions of up to 35% can be reached in the low-energy house with a PVT area of 40 m².
- In the passive house, electric solar fractions of up to 80% can be reached with a PVT area of 50 m² and a battery storage capacity of 30 kWh, while electric solar fractions of up to about 70% can be reached in the low-energy house with a PVT area of 50 m² and a battery storage capacity of 30 kWh.
- The solar thermal output is directly connected to the heat pump evaporator. Thus, the solar thermal output depends solely on the energy consumption of the house/heat pump operation and is not influenced by the tilt and the area of the PVT

5.6 Office building in Beijing, cold and temperate climate (China)

5.6.1 Building and System

Table 14 shows building and system data used as the starting point of the simulations and study. In chapter 5.6.3 all variants are listed.

Table 14: Building and system data for Office building

Building Data	
Location	Beijing (China)
Building	Office building

Energy ref. area	2,850 m² (NFA)	
Useful energy (Q_{cons} and E_{cons})		
Heating demand	44.16 kWh/(m²a)	
Cooling demand	30.63 kWh/(m²a)	
DHW demand	2.46 kWh/(m²a)	
Electricity demand for equipment and lighting	33.41 kWh/(m²a)	
E-mobility demand	- kWh/(m²a)	
Total heating demand	46.62 kWh/(m²a)	
Total electricity demand	47.65 kWh/(m²a)	
Final energy (Qf)	47.65 kWh/(m²a)	
System Data		
Heating generator	Municipal thermal grid (gas boiler)	
Cooling generator	Split air-conditioner	
PV	Total area Number of modules (placed) System efficiency (including all periphery) Peak power	~ 1,456.00 m² 278 pieces of sc-Si PV panels with 400Wp rated power applied on the roof by 5° inclination towards south; 224 pieces of CdTe thin film PV panels with 100Wp rated power applied on the roof horizontally; 469 pieces of CdTe thin film PV panels with 100Wp rated power applied on the roof by 5° inclination; 313 pieces of CdTe thin film PV panels with 100Wp rated power applied on south façade paralleled with the wall; 70 pieces of CdTe thin film PV panels with 100Wp rated power applied on west façade paralleled with the wall; 110 pieces of CdTe thin film PV panels with 100Wp rated power applied on east façade paralleled with the wall; 14 pieces of transparent CdTe thin film PV panels (70% light transmittance) with 154 Wp rate power applied on south facade paralleled with the curtain wall. 16.53 % for sc-Si PV system, 11.39% for CdTe thin film PV system, and 3.42% for CdTe thin film PV system with 70% light transmittance. 232 kWp
Solar thermal	Total area Total aperture area Thermal capacity Collector type	- m² - m² - W -
Thermal storage	Volume	-

Electrical storage	Capacity Storage type	-
Ventilation system	System Air change Heat recovery	Natural ventilation / windows - 1/h - %
Heating system	Municipal thermal grid	
DHW preparation	Electric water heater	
Cooling system	Split air conditioner	

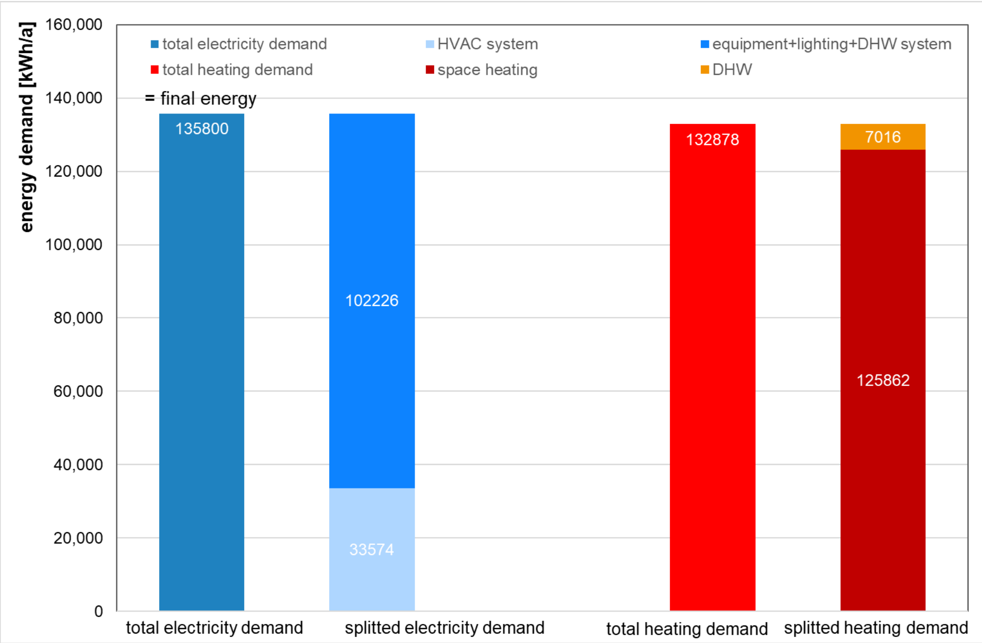

Figure 44: Electricity demand and demand of thermal energy of the building

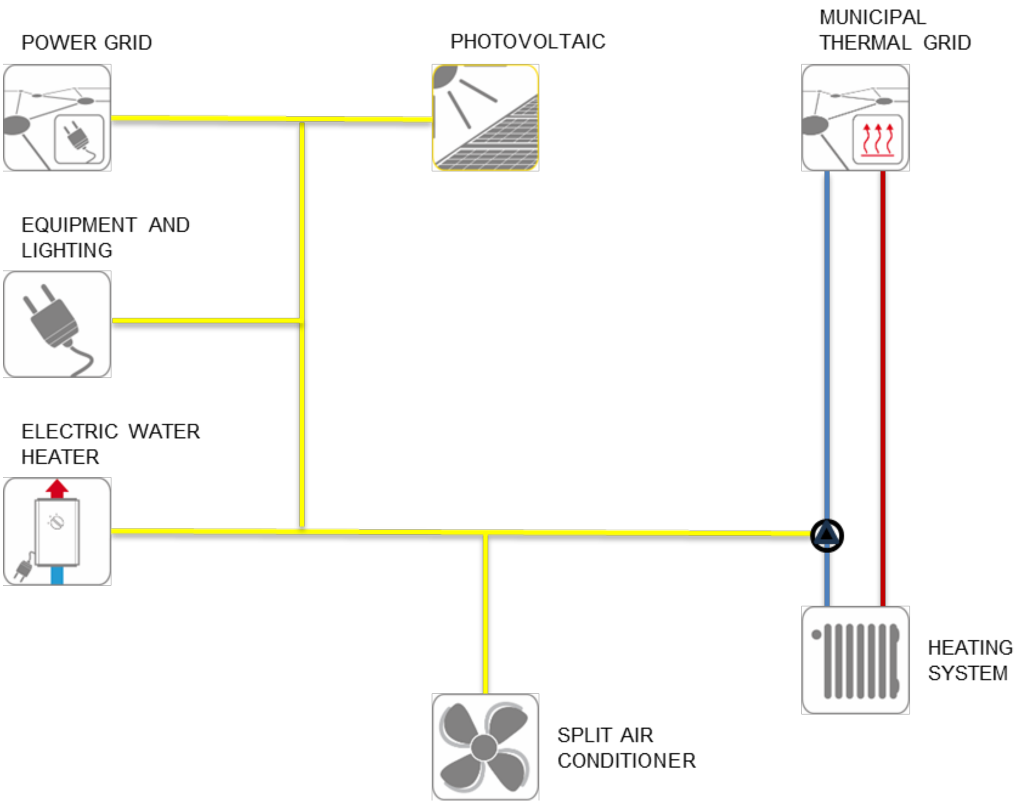

Figure 45: energy concept and systems

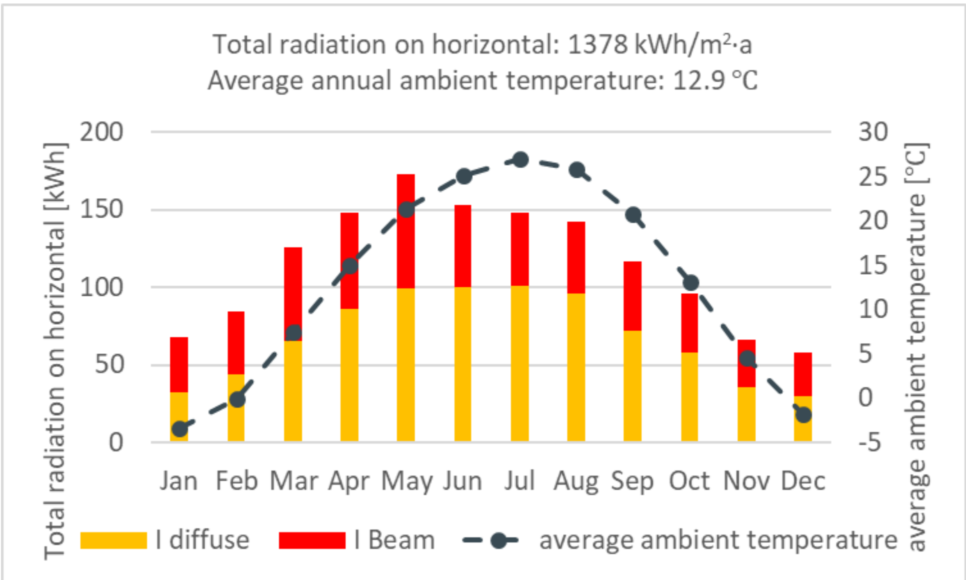

Figure 46: Weather data Beijing (China), average ambient temperature and solar radiation on horizontal

5.6.2 System management philosophy/control strategy

The office building is connected to the municipal thermal grid. And the heating season is from 15th, Nov to 15th, Mar the next year. The indoor temperature is set at 18 ℃ in heating season. When the indoor temperature can not meet the set value in rare cases, the split air-conditioner can be used as a supplementary heat source, and it can independently operate according to user demand. Natural ventilation via the windows is possible at all times. A photovoltaic system is provided to support the power supply. The remaining electricity required for building operation is drawn from the public grid.

If the PV power is not sufficient, electricity is supplied from the grid. The domestic hot water is provided by electric water heater.

5.6.3 Simulation variations

In the process of building renovation, both renewable energy application and building energy efficiency are considered. In south façade of the building, the PV shading is applied to increase total installed capacity of PV system and at the same time reduce the solar heat gain from the window in summer. Hence, the energy consumption of air conditioner can be saved. The building applies multiple kinds of PV systems to study the different power generation performance of PV systems under different kinds, orientations, inclinations conditions. For carrying out the simulation study, the simulation variants are set below. (see Table 15)

Table 15: Simulation variants

Variation	Starting point	Changes/ adaptions
PV shading	With PV shading	Without PV shading
PV types	Sc-Si PV system	CdTe thin film PV system
Orientation of PV	South	Horizontal West east
Inclination of PV	Horizontal	5° , orientation south 90° , orientation south

5.6.4 Results

5.6.4.1 Influence of PV shading

The ZEB demo case was converted from an existing building which was built in 1970s. To increase the application of photovoltaic system and realizing building energy efficiency at the same time, the ZEB applied PV shading on south facade. As figure 5 shown, after applying the PV shading system, the building space heating demand increased slightly, and the cooling demand decreased efficiently, which lead a decrease in total energy demand of the building. In consideration of that the ZEB is connected to municipal thermal grid for space heating, the total electricity demand only includes equipment, lighting, cooling system and electric DHW system parts. So, the total electricity demand decreases.

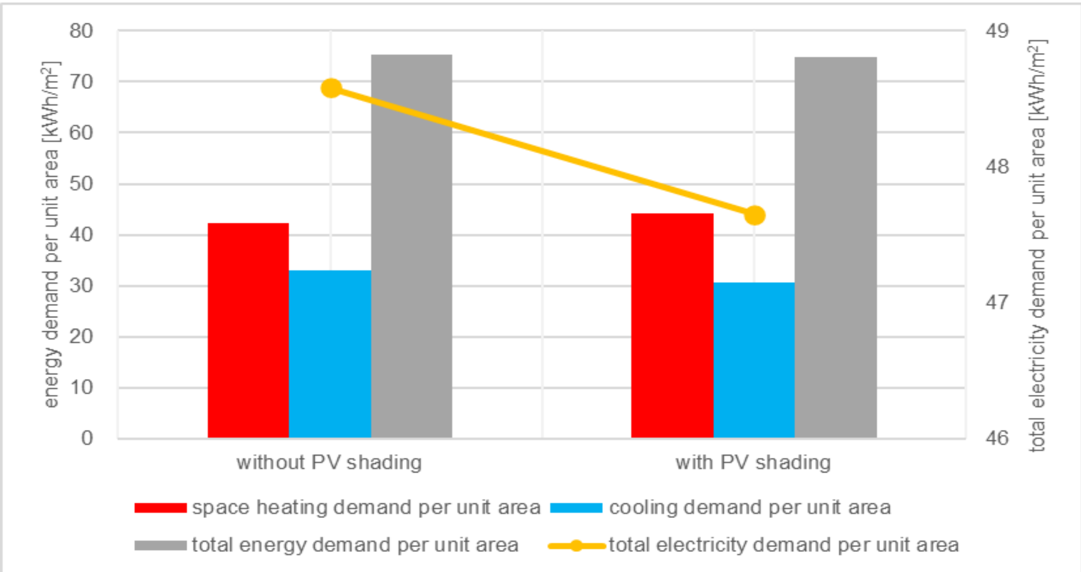

Figure 47: Energy demand and electricity demand – PV shading system

5.6.4.2 Influence of photovoltaic type on power generation

The ZEB demo case applied 2 kinds of photovoltaic systems, which includes sc-Si photovoltaic system and CdTe thin film photovoltaic system (also applies a little part of transparent PV panels with 70% light transmittance), on different building surfaces. Hence, the whole building photovoltaic system is divided into 10 sub-systems to help to study the operation performance of each kinds of photovoltaic systems. Figure 6 compares the power generation difference between the sc-Si photovoltaic system and the CdTe thin film photovoltaic system on the roof with a 5° inclination toward the south.

It can be seen from the figure 6 that the power generation of sc-Si photovoltaic system is significantly higher than that of CdTe thin film photovoltaic system with the same inclination for having higher photoelectric conversion efficiency. However, from the equivalent full sun hours aspect, it presents a opposite trend. That is because the CdTe thin film photovoltaic system have a wider spectral absorption range than sc-Si photovoltaic system, which can help it show a better power generation ability in low light condition.

Figure 48: Power generation and equivalent full sun hours of sc-Si photovoltaic system and CdTe thin film photovoltaic system by the same inclination on the roof

5.6.4.3 Influence of orientation and tilt angle of photovoltaic systems

The CdTe thin film photovoltaic system is applied on building facades in a large scale. The applied orientation includes south, west, and east. So the Figure 52 compares the power generation performance and equivalent full sun hours in different orientation of CdTe thin film photovoltaic systems. As the figure show that the power generation of photovoltaic system on roof is the most, And then is on south façade. The power generation of photovoltaic system on west and east façade is nearly the same. The power generation characteristic presents the same trend with the situation of solar radiation received by each surface of the building.

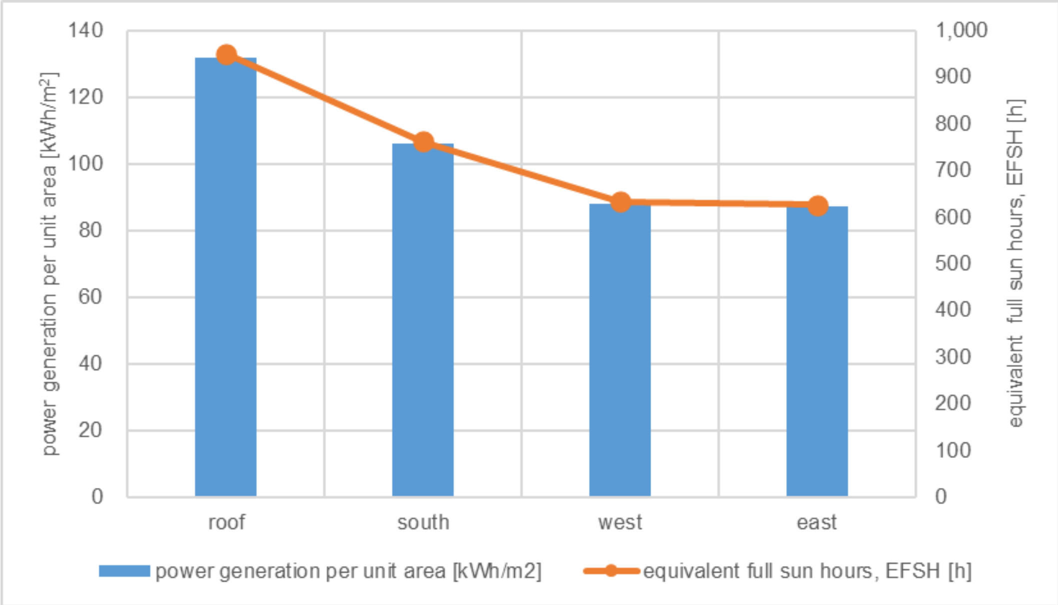

Figure 49: Power generation and equivalent full sun hours – orientation of CdTe thin film photovoltaic systems

Also, for rooftop photovoltaic system, the Figure 53 shows the variation of power generation in different inclinations. Along with the increasing inclination, the power generation shows a trend of increasing first and then decreasing. The power generation will reach peak when the photovoltaic panel located in optimum inclination, which is about 30° in Beijing.

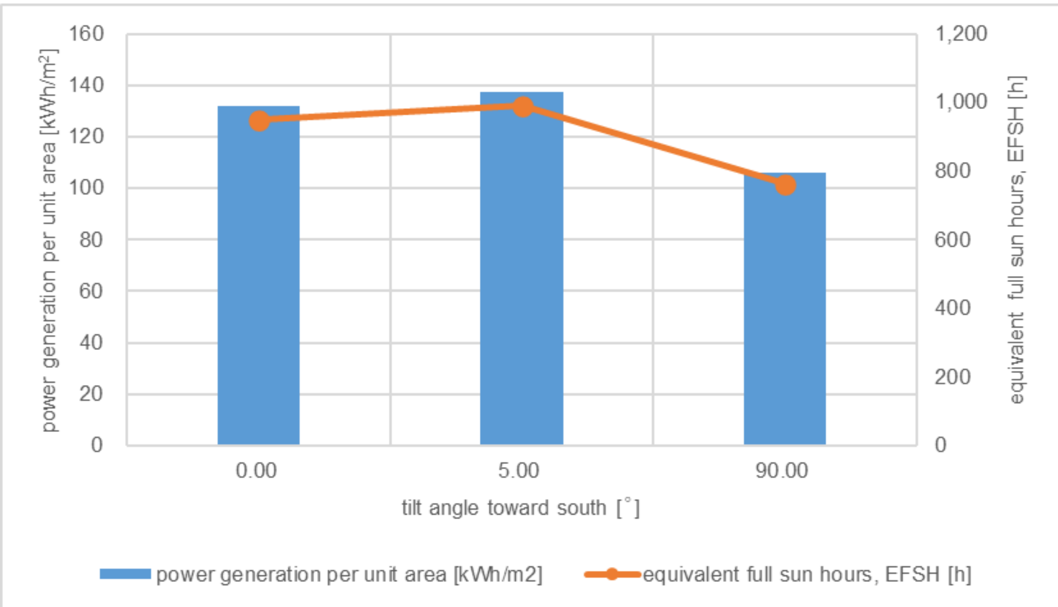

Figure 50: Power generation and equivalent full sun hours – inclination of CdTe thin film photovoltaic systems toward south

5.6.5 Conclusion – Outcomes

Outcome of the variants for reaching SEB:

- PV modules should be applied in building roof and arranged in a southward inclination as priority. PV with a small inclination angle can ensure the power generation while making full use of the roof area.
- The efficiency and area of PV should be as high as possible.

PV used in building façade should be combined with building functional component, such as shading etc. While considering power generation, it can reduce the energy demand of building.

5.7 Residential/Single dwelling (Josh's House), warm temperate climate (Australia)

5.7.1 Building and System

Josh's House (Byrne, 2024) was built in 2013 as a national exemplar of energy efficient dwelling design for the volume market. With the addition of an electric vehicle (EV) and a recent update to the solar energy system (mid-2018), this applied study continued in conjunction with local business partners. The original gas-boosted solar hot water system was replaced with an electric heat pump, and the gas stove was replaced with an induction cooktop, making the home totally solar-electric. The new appliances, as well as the EV charging station, are metered, and the data provides useful insights into the effect of auto charging on a solar-electric household. Josh's House received 10/10 stars from the Nationwide House Energy Rating Scheme (NatHERS) and is a net energy exporter. It collects and recycles most of its own water, and landscaping includes food production, wildlife habitat, and play spaces. The interiors incorporate 'Healthy Homes' (indoor air quality) and 'Livable Homes' (universal access) principles

Table 16: Building and system data for Residential/Single dwelling in Australia

Building Data		
Location	Perth (WA, Australia)	
Building	Residential/Single dwelling	
Energy ref. area	122 m²	
Useful energy (Q_{cons} and E_{cons})		
Heating demand	* Not specifically measured, see Appliance demand	
Cooling demand	* Not specifically measured, see Appliance demand	
DHW demand	-	
Household demand	Appliances: 15.71 kWh/(m²a); Lighting: 2.70 kWh/(m²a); Cooking (induction): 0.87 kWh/(m²a); Bore pump (auxiliary): 1.40 kWh/(m²a); Gray water pump (auxiliary): 0.08 kWh/(m²a); Rainwater pump & UV treatment: 3.75 kWh/(m²a);	
E-mobility demand	7.11 kWh/(m²a)	
Total heating demand	-	
Total electricity demand	37.93 kWh/(m²a)	
Final energy (Qf)	37.93 kWh/(m²a)	
System Data		
Heating generator	Not described specifically	
Cooling generator	Not described specifically	
PV	Total area	32.5 m²
	Number of modules (placed)	18 modules on the roof
	System efficiency (including all periphery)	20 % at STC (Manufacturer info)

	Peak power	6.4 kWp
Solar thermal	Total area Total aperture area Thermal capacity Collector type	-
Thermal storage	Volume	-
Electrical storage	Capacity Storage type	- Total 9.8 kWh; Usable 8.8 kWh - Lithium-ion
Ventilation system	System Air change Heat recovery	-
Heating system	-	
DHW preparation	-	
Cooling system	-	

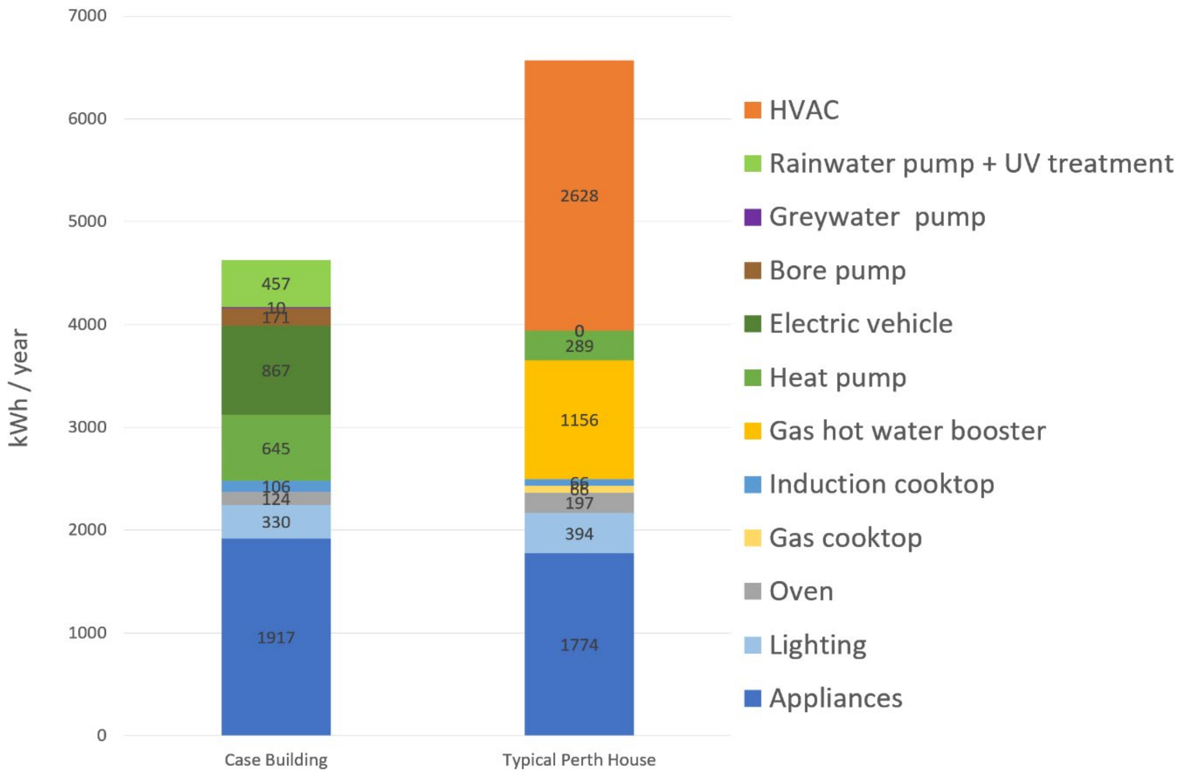

Figure 51: Electricity demand breakdown and comparison to typical house in Perth, WA, Australia

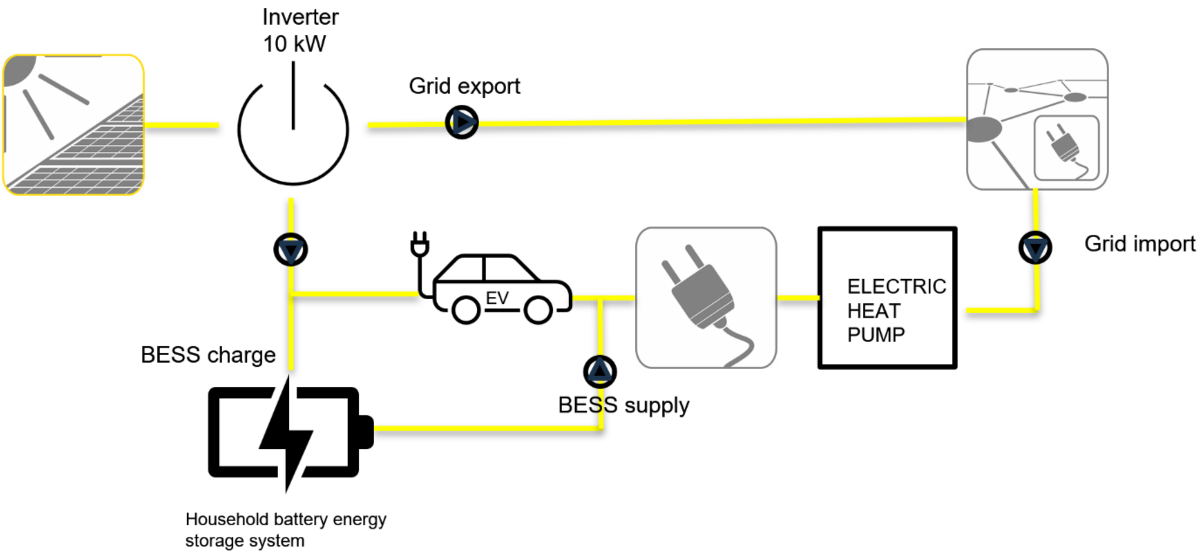

Figure 52: energy concept and systems

5.7.2 System management philosophy/control strategy

The demonstrated case of Josh's house is a fully electrified residential dwelling in Perth, Australia. The building is powered by a 6.4 KW rooftop PV system, the public grid, and battery energy storage with a usable capacity of 8.8 kWh. The PV generation will prioritize the demand of household appliances including a hot water heat pump and EV charging, while the excessive solar generation will be used to charge the battery system. If the demand is fully offset and the battery reaches its maximum capacity, the rest of the PV generation will be fed into the public grid.

5.7.3 Simulation variations

The simulation process recreates the processes of PV-load-BESS-grid interaction of the case building to evaluate its performance on offsetting the electricity load using the PV and battery systems.

Table 17: Simulation variants

Variation	Starting point	Changes/ adaptions
PV system tilt angle (°)	As build tilt angle (24.5° as of the roof tilt)	24.5° to 40° with 4 degrees interval
Share of PV system on rooftop surface (%)	As build PV share on rooftop (32.5 m^2 / 65% coverage)	55% to 80% share on rooftop surface with 5% interval

5.7.4 Results

5.7.4.1 Comparison between simulation and measurement records

The simulation was carried out using SIMULINK and MATLAB. A PV performance evaluation model was developed based on the Sandia National Lab's PVlib toolbox (Holmgren et al., 2018). The measurement data was provided by the house owner, which comprise of the smart-metering data of the PV AC power from inverter and the national metering identifier (NMI) data of the electricity usage in the year of 2018. Due to the data availability, roughly two months' data was missing (June and July 2018).

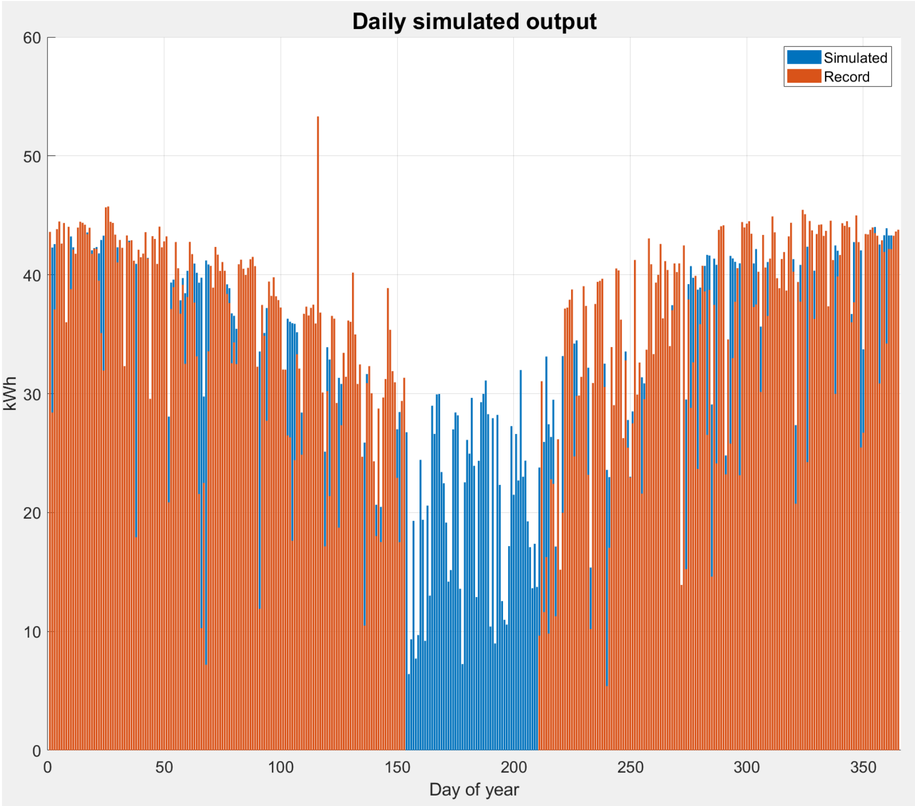

Figure 53: Daily electricity generation from PV system (kWh)

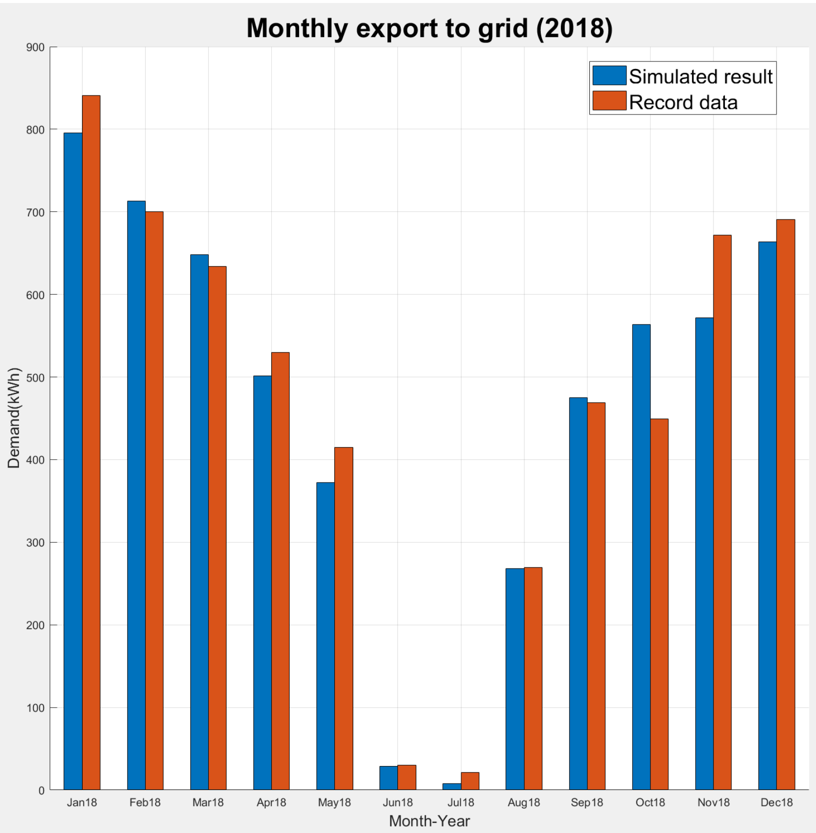

Figure 54: Monthly export of electricity to the public grid (kWh)

Figure 53 and Figure 54 compare simulated and recorded data, where Figure 53 is the daily electricity generation (kWh) over the year, and Figure 54 is the monthly exported electricity (kWh) to the public grid. The simulation results shown in Figure 53 and Figure 54 use the same settings of the as-build system as outlined in *Table 16*. The key components simulated include the grid-connected PV and BESS systems with a 10-kW inverter. Although the simulated results cannot fully represent the record data, they can provide the pattern of PV generation and interaction between PV, BESS, and public grid with a reasonable similarity.

5.7.4.2 Influences of angular and coverage ratio settings

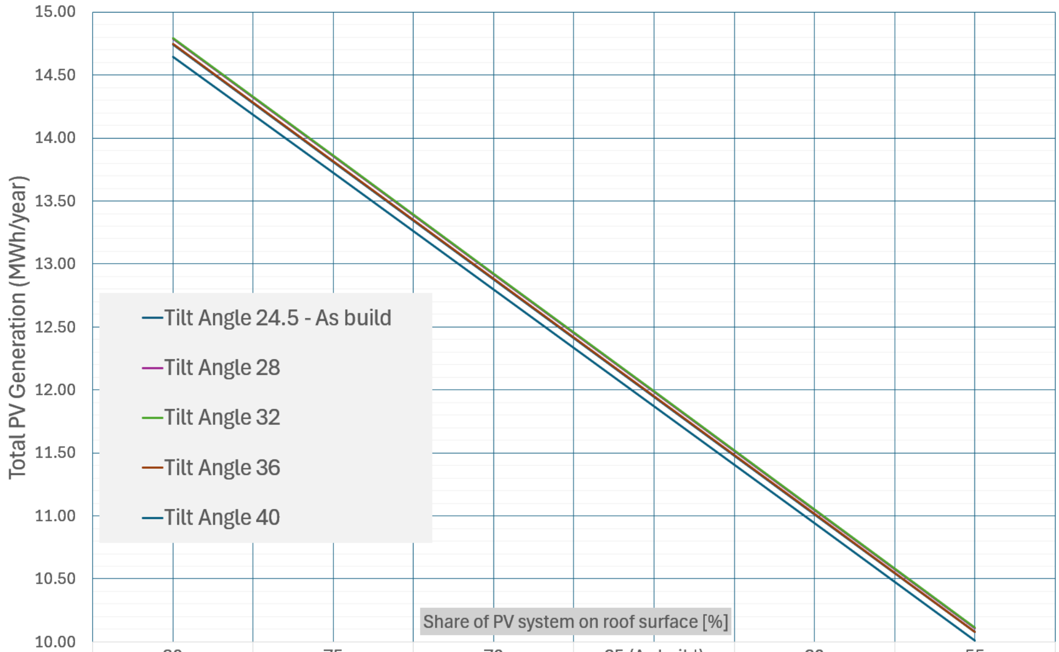

	80	75	70	65 (As build)	60	55
Tilt Angle 24.5 - As build	14.7407	13.8099	12.8783	11.9457	11.0123	10.0780
Tilt Angle 28	14.7871	13.8535	12.9190	11.9836	11.0473	10.1101
Tilt Angle 32	14.7917	13.8578	12.9230	11.9873	11.0508	10.1133
Tilt Angle 36	14.7452	13.8142	12.8823	11.9495	11.0158	10.0812
Tilt Angle 40	14.6459	13.7210	12.7953	11.8686	10.9411	10.0127

Figure 55: Impacts on annual total PV generation (MWh/year)

Figure 55 illustrates the impact of PV coverage on the roof surface and the tilt angle options on the total yearly generation of the PV system. Among the tested angles, a tilt of 32° yields the highest annual PV generation, while the as-built option (24.5°) is suboptimal. However, it is noteworthy that the deviation from the ideal tilt angle reduces annual generation by less than 0.4%.

Moreover, the share of rooftop coverage by the PV system plays a more substantial role in determining PV generation. There is a positive linear correlation between the PV coverage ratio and the annual PV generation. However, for residential buildings, achieving a coverage ratio above 80% may be challenging due to architectural constraints, such as structural obstructions (e.g., vents, skylights, antennas), wind loading, and structural integrity considerations.

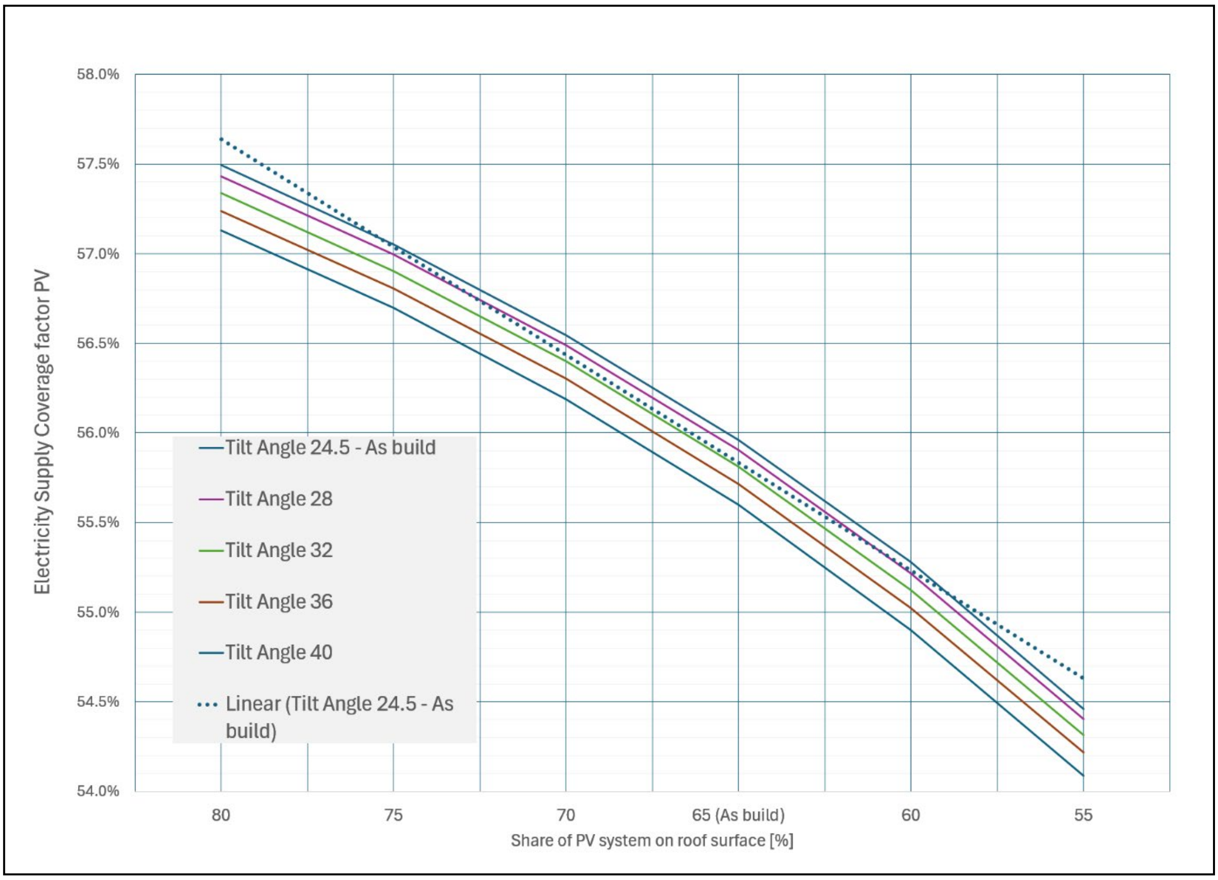

Figure 56: Impacts on electricity supply coverage factor (%)

Figure 56 illustrates the effects of PV coverage on the roof surface and tilt angle options on the electricity supply coverage factor. It is observed that tilt angles ranging from 24.5° to 40° have minimal impact on the supply coverage factor, with less than a 0.5% variance across the different options. Interestingly, although the 32° tilt angle yields the highest generation, as shown in Figure 6, the as-built option (24.5°) results in the highest demand offset ratio, as demonstrated in Figure 56. This discrepancy may be attributed to better generation-demand matching at the 24.5° angle compared to the 32° angle.

Regarding the PV system's coverage on the roof surface, the increase in the supply coverage factor does not follow a linear correlation with the rise in the roof coverage ratio. The growth rate of the supply coverage factor is higher when the coverage ratio is below 60%, but it slows when the ratio exceeds 75%. This could be due to the limitations of the Battery Energy Storage System (BESS), as the BESS capacity restricts further increases in the supply coverage factor even as PV generation rises with higher coverage ratios.

5.7.4.3 Conclusion – Outcomes

- Rooftop PV systems combined with BESS provide a practical solution for fully electrifying residential dwellings.
- While the angular design of the PV system impacts both demand offset and power generation, the variations between different angles are minimal for single dwellings, allowing for greater flexibility in the architectural and structural design of the rooftop.
- Although higher rooftop coverage ratios offer increased energy generation and flexibility, solar deployments on residential rooftops must also account for the detailed design of rooftop features and the structural integrity of the building.
- Effective generation and demand matching is essential, underscoring the importance of a BESS. Moreover, integrating a BESS creates opportunities to explore additional solutions, such as smart energy management systems, to further optimize energy efficiency.

5.7.4.4 References

Byrne, J. (2024). *Josh's House: Showcasing the benefits of sustainable housing to the community through demonstration and inspiration*. https://joshshouse.com.au/

Holmgren, W., C, H., & Mikofski, M. (2018). pvlib Python: A python package for modeling solar energy systems. *Journal of Open Source Software*, *3*(29), 884.